SYNTHESIS AND CHARACTERIZATION OF CERIA-NICKEL MIXED OXIDE SOLID SOLUTION

MS. PIYANATH YUTHARAT

MS. PORNRIN JINTANAVASAN

MS. PIMPLOY RUTHCHASANEE

A SPECIAL PROJECT SUBMITTED IN PARTIAL FULFILLMENT

OF THE REQUIRMENT FOR THE DEGREE OF BACHELOR OF SCIENCE

IN PETROCHEMICAL TECHNOLOGY (INTERNATIONAL PROGRAM)

FACULTY OF SCIENCE

KING MONGKUT'S INSTITUTE OF TECHNOLOGY LADKRABANG

ACADEMIC YEAR 2010

SYNTHESIS AND CHARACTERIZATION OF CERIA-NICKEL MIXED OXIDE SOLID SOLUTION

MS. PIYANATH YUTHARAT

MS. PORNRIN JINTANAVASAN

MS. PIMPLOY RUTHCHASANEE

A SPECIAL PROJECT SUBMITTED IN PARTIAL FULFILLMENT

OF THE REQUIRMENT FOR THE DEGREE OF BACHELOR OF SCIENCE

IN PETROCHEMICAL TECHNOLOGY (INTERNATIONAL PROGRAM)

FACULTY OF SCIENCE

KING MONGKUT'S INSTITUTE OF TECHNOLOGY LADKRABANG

ACADEMIC YEAR 2010

Title	Synthesis and characterization of ceria – nickel mixed oxide solid solution
Students	Ms. Piyanath Yutharat
	Ms. Pornrin Jintanavasan
	Ms. Pimploy Ruthchasenee
Degree	Bachelor of Science
Major Program	Petrochemical Technology
Academic Year	2010
Advisor	Assoc.Prof.Dr.Somsak Woramonkolchai
Co-Advisor	Assoc.Prof.Dr.Thirasak Rirksomboon

ABSTRACT

The aims of this research are to prepare and characterize the $Ce_{1-x}Ni_xO_2$ mixed oxide solid solution catalysts with varying mole ratio (x = 0.25, and 0.75). The catalysts were prepared via co – precipitation and urea hydrolysis methods. The catalysts were calcined at the temperature of 550 ^{o}C under same condition in both methods. Many characterization techniques which including TGA, SEM, XRF, XRD, and TPR were used to determine the structures and the properties of the catalysts.

The results showed that the catalysts were consisted of NiO and CeO_2; both are in the crystalline phase. The TGA results indicated that the temperature at 550 $^{\circ}$C was the lowest temperature for the calcinations of the $Ce_{1-x}Ni_xO_2$ mixed oxide catalysts. From SEM technique, the increasing in the Ni loading affected the Ni dispersion on the ceria surface. The elemental compositions of the catalysts were characterized by the XRF technique. The results from the XRD indicated that ceria (CeO_2) was a cubic fluorite structure. The reduction temperature of the catalysts was achieved from the TPR technique; it was shown that the increasing in Ni loading was no significant of effect on the reduction temperature of NiO over CeO_2.

Keywords: $Ce_{1-x}Ni_xO_2$; solid solution; co – precipitation; urea hydrolysis

Acknowledgement

This special project is owned by King Mongkut's Institute of Technology Ladkrabang under cooperation with Department of Chemical Technology and Chulalongkorn University.

Firstly, we would like to dedicate all benefits to our advisors Assoc.Prof.Dr.Somsak Woramonkolchai; Faculty of Science King Mongkut's institute of technology Lardkrabang and co-advisor, Assoc. Prof.Dr.Thirasak Rirksomboon; The Petroleum and Petrochemical College, Chulalongkorn University for all suggestion and useful information.

We would like to thank the committees, Dr.Samart Kongtaweelert, Dr.Pisek Rungrojchaipon, Dr.Naratip Vittayakornand Dr.Montree Thongkam; Faculty of Science KMITL for their special suggestions and comments. And also thank for all professors in Department of chemistry; Faculty of Science KMITL.

Thanks you to all of KMITL science stuffs for providence instrument and chemicals in all laboratory workplace.

Finally, we would like to thank our adorable families and all our friends for their support, encouragement, love and concern along this special project.

Miss Piyanath Yutharat

Miss Pornrin Jintanavasan

Miss Pimploy Ruthchasenee

Table of Contents

Table of Contents (Cont.)

Page

Table of Contents (Cont.)

Page

Table of Contents (Cont.)

Page

List of Tables

List of Figures

Figure Page

List of Figures (Cont.)

Figure Page

Chapter 1

Introduction

1.1 Motivation

Currently fossil fuels, non-renewable resources, are the most economically available sources of power for both personal and commercial uses. To release their stored energy, fossil fuels must be burned. In a combustion process, a variety of emissions and particulates are released into the atmosphere. Primary releases are sulfur, nitrogen, and carbon, which can be harmful to the environment. Especially carbon dioxide (CO_2), a greenhouse gas, which is a key factor in global warming [1].

Hydrogen production is one of the most attractive ways to produce the energy which will reduce the greenhouse gas emissions and the atmospheric pollution [2]. Steam reforming of methane, the natural gas, can be used to produce hydrogen as follows:

$$CH_4 + CO_2 \rightleftharpoons 2CO + 2H_2, \quad \Delta H_{298} = +247.3 \text{ kJ mol}^{-1} \qquad (1.1)$$

However, this reaction is endothermic reaction which occurs in high temperature (> 800 °C) and consumes more energy. Partial oxidation of methane offers the greatest potential to hydrogen or synthesis gas due to mild exothermicity, high conversion, suitable H/C ratio and a very short residence time as shown in equation [3]:

$$CH_4 + 1/2O_2 \rightarrow + CO + 2H_2, \quad \Delta H_{298} = -35.6 \text{ kJ mol}^{-1} \qquad (1.2)$$

The key component in this process is the catalysts. They can be classified in two groups: noble metals (Pt, Pd, Rh), and transition metal oxides (Ni, Co, Fe). Although transition metal oxides are less active than noble metals, they are used in industrial application due to their low cost [4]. The Ni-based catalyst is widely used due to its high activity and selectivity and also its low cost. But the most important problem is that nickel can be deactivated due to carbon deposition or metal loss at high temperature [5].

Ceria (CeO_2) has been widely used as a promoter and an oxidation catalyst because of its unique redox properties and high oxygen storage capacity [6, 7]. It has been reported that CeO_2 has potential uses for the removal of post-combustion pollutants, for the removal of organics from wastewater (catalytic wet oxidation) and in fuel cell technology [7]. In association with other catalysts, ceria can effectively reduce NO_x emissions as well as convert harmful carbon monoxide to the less harmful carbon dioxide [8].

To improve the nickel catalytic activity and thermal stability, ceria should be added as the support. Ceria not only stabilizes the support but also stores and releases oxygen under oxidation and reduction condition, respectively.

In this study, we attempted to compare $Ce_{1-x}Ni_xO_2$ prepared by urea hydrolysis and co-precipitation methods under the same conditions. In urea hydrolysis method the molar ratio of Ce/Ni was separated into two sets; set 1) is $Ce_{0.75}Ni_{0.25}$ and set 2) is $Ce_{0.25}Ni_{0.75}$. The catalysts should be calcined at 550 °C for 6 hours. Then do the same condition in co-precipitation method. Thermogravimetric Analysis (TGA) was used to determine changes in weight in relation to change in temperature and optimal temperature in calcination. Scanning electron microscope (SEM) was used to observe the morphology of the catalyst. The elemental composition was obtained from X-ray fluorescence (XRF). X-ray diffractometer (XRD) was used to identify the different phase in the catalyst and determine its crystallinity. And TPR was used to study the reducibility of NiO after calcined.

1.2 Objective

1. To study the performance of the catalysts with different $Ce_{1-x}Ni_xO_2$ when x = 0.25 and 0.75, respectively under the same conditions.
2. To study the influence of the preparing methods to the performance of the catalysts.
3. To study the characters of synthesized ceria-nickel mixed oxide catalysts that can be properly used in methane partial oxidation reaction.

1.3 Scope of study

1. To synthesize ceria-nickel mixed oxide solid solution.
2. To study the characters of the catalysts prepared with the different methods under the same conditions.
3. Characterization of ceria-nickel catalysts
   - 3.1 Thermogravimetric Analysis (TGA)
   - 3.2 Scanning electron microscope (SEM)
   - 3.3 X-ray fluorescence (XRF)
   - 3.4 X-ray diffraction (XRD)
   - 3.5 H_2-temperature programmed reduction (H_2-TPR)

1.4 Expected result

1. To be able to synthesize the ceria-nickel mixed oxide solid solution.
2. To understand the principle of the preparation methods; co-precipitation and urea hydrolysis methods.
3. To understand the mole ratio and the preparation methods which are the factors that affect the catalysts.
4. To be able to apply the knowledge from this research for further study.

Chapter 2

Theory and Literature review

2.1 Catalyst

A catalyst can be defined as a substance that increases the rate of a chemical reaction. A catalyst can be synthetic, organic or simply a metal. The process through which a particular catalyst increases the rate of a particular reaction is called as catalysis. Actually, for occurrence of any process, an energy, which is called as activation energy is always required. For reactants of every reaction, it's a necessity to achieve this activation energy, to get converted into the final products. This energy barrier of a reaction is called as activation energy barrier. For reactants alone, it is very tedious to achieve this barrier. But when a catalyst is present in a particular reaction it decreases the activation energy barrier. So, reaction occurs at a faster rate than before. A catalyst speeds up a reaction by changing the specific structures of the reactant molecules; this alteration causes reactant molecules to collide with each other in order to release energy or product. There are some negative catalysts also, which decreases the rate of a well- going reaction. These negative catalysts interfere with the normal functioning of usual catalysts of a particular reaction. Negative catalysts can also be termed as inhibitors. These negativecatalysts have great uses in medical science. They help in slowing down of various detrimental biochemical reactions [9].

Substances that reduce the action of catalysts are called catalyst inhibitors if they were reversible, and catalyst poisons if they were irreversible. Promoters are substances that increase the catalytic activity, particularly when not being catalysts unto themselves. The inhibitor may modify selectivity in addition to rate. For instance, in the reduction of ethyne to ethene, the catalyst is palladium (Pd) partly "poisoned" with lead (II) acetate ($Pb(CH_3COO)_2$). Without the deactivation of the catalyst, the ethene produced will be further reduced to ethane. The inhibitor can produce this effect by e.g. selectively poisoning only certain types of active sites. Another mechanism is the modification of surface geometry. For instance, in hydrogenation operations,

large planes of metal surface function as sites of hydrogenolysis catalysis while sites catalyzing hydrogenation of unsaturated are smaller. Thus, a poison that covers surface randomly will tend to reduce the number of uncontaminated large planes but leave proportionally smaller sites free, thus changing the hydrogenation vs. hydrogenolysis selectivity. Many other mechanisms are also possible.

Promoters can cover up surface to prevent production of a mat of coke, or even actively remove such material (e.g. rhenium on platinum in platforming). They can aid the dispersion of the catalytic material or bind to reagents.

2.1.1 Type of catalysis

1. Heterogeneous catalysts

Heterogeneous catalysts act in a different phase than the reactants. Most heterogeneous catalysts are solids that act on substrates in a liquid or gaseous reaction mixture. Diverse mechanisms for reactions on surfaces are known, depending on how the adsorption takes place. The total surface area of solid has an important effect on the reaction rate. The smaller the catalyst particle size, the larger the surface area for a given mass of particles.

Heterogeneous catalysts are typically "supported," which means that the catalyst is dispersed on a second material that enhances the effectiveness or minimizes their cost. Sometimes the support is merely a surface on which the catalyst is spread to increase the surface area. More often, the support and the catalyst interact, affecting the catalytic reaction. Supports are porous materials with a high surface area, most commonly alumina or various kinds of carbon. Specialized supports include silicon dioxide, titanium dioxide, calcium carbonate, and barium sulfate.

2. Homogeneous catalysts

Homogeneous catalysts function in the same phase as the reactants, but the mechanistic principles invoked in heterogeneous catalysis are generally applicable. Typically homogeneous catalysts are dissolved in a solvent with the substrates. One example of homogeneous catalysis involves the influence of H^+ on the esterification of esters, e.g. methyl acetate from acetic acid

and methanol. For inorganic chemists, homogeneous catalysis is often synonymous with organometallic catalysts.

3. Electrocatalysts

In the context of electrochemistry, specifically in fuel cell engineering, various metal-containing catalysts are used to enhance the rates of the half reactions that comprise the fuel cell. One common type of fuel cell electrocatalyst is based upon nanoparticles of platinum that are supported on slightly larger carbon particles. When in contact with one of the electrodes in a fuel cell, this platinum increases the rate of oxygen reduction to water, either to hydroxide or hydrogen peroxide.

4. Organocatalysis

Whereas transition metals sometimes attract most of the attention in the study of catalysis, organic molecules without metals can also exhibit catalytic properties, as is apparent from the fact that many enzymes lack transition metals. Typically, organic catalysts require a higher loading (or amount of catalyst per unit amount of reactant) than transition metal-based catalysts, but these catalysts are usually commercially available in bulk, helping to reduce costs. In the early 2000s, organocatalysts were considered "new generation" and are competitive to traditional metal-containing catalysts. Enzymatic reactions operate via the principles of organic catalysis [10].

2.1.2 Support metal catalyst

In the chemicals industry, the majority of the reactions take place at the surfaces of heterogeneous catalysts. The efficiency of a heterogeneous catalytic process is thus largely determined by the quality of the catalysts used, i.e. the exposed surface area of active phase and the stability.

It is instructive to show the correlation between the exposed (specific) surface area, and the particle size of the catalytic material. Let us suppose that the active phase (density ρ in kg/m^3) consists of uniform spherical particles. The specific area can be calculated as follows:

Volume of one particle, $V = 1/6\pi d^3$ (m^3)

Weight of one particle, $W = 1/6\rho\pi d^3$ (kg)

Surface area of one particle, $Sp = \pi d^2$ (m^2)

Specific surface area, $SA = Sp/W = \pi d^2/(\rho 1/6\pi d^3) = 6/\rho d$ (m^2/kg)

As an example, nickel has been chosen. It is obvious that only at low values of the particle sizes (1–10 nm) are reasonable surface areas obtained. It is impossible to apply such small particles in reactors, and therefore support bodies are applied. Catalyst supports are in general porous materials, so as to allow a high loading of highly dispersed metal particles, while the particles of the active phase usually need to be synthesized in such a way that they are as small as possible.

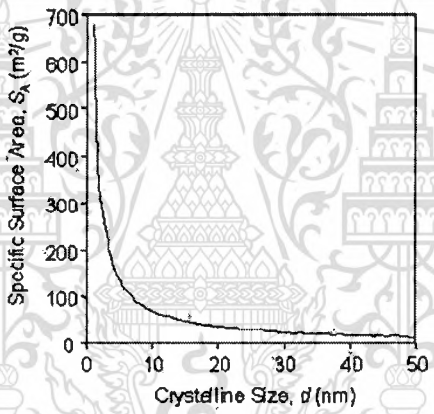

Figure 2.1 A plot of specific area calculation[11].

Despite the observations made above, many authors of papers in catalysis journals seem to ignore the importance of the preparation procedure used for the eventual catalytic results they obtain.

The procedure used is usually described in very general terms, and often conditions that appear to have no fundamental reasoning are used, e.g. the used catalyst precursor, calcinations conditions, pH of precursor solution (often not mentioned), temperature of solutions, etc. Fortunately, other researchers take the preparation of catalysts seriously and many publications and text-books exist that discuss the preparation of catalysts on a scientific basis.1 Especially in the group of Geus (now De Jong) at the Utrecht University in The Netherlands,1,2 years of research on the preparation of catalysts has lead to a more scientific basis for catalyst preparation.

Several procedures exist in order to attach the active phase to the support, i.e. to prepare supported catalysts. In the catalyst manufacturing industry, impregnation is usually employed for practical and economic reasons. Impregnation allows the use of pre-shaped or structured supports. Preparation of catalysts starting from these commercially available supports is attractive because a support with optimal properties can be selected.

From a chemical point of view, impregnation and precipitation represent two extreme cases:

- Impregnation which is often related to ion exchange, where the interaction with the support is dominant; or
- Precipitation which in principle is a crystallization process and can occur in the bulk of the liquid or on a relatively inert surface. Here, particles of active phase can be kept small because the support particles act as crystallization nuclei for the active phase precursor.

The most common techniques for preparation of supported metal catalysts will be discussed, including impregnation, co-precipitation, homogeneous deposition precipitation, and precipitation at Constant pH. In principle, these techniques can all be used to attach the active phase to supports, some preferably in the form of a powder, others in the form of a pre-shaped body [11].

2.2 Cerium(IV)oxide also known as ceria oxide, ceria, cerium oxide or cerium dioxide, is an oxide of the rare earth metal cerium. It is a pale yellow-white powder with the chemical formula CeO_2. Cerium (IV) oxide is formed by calcining cerium oxalate or cerium hydroxide. Powdered ceria is slightly hygroscopic and will also absorb a small amount of carbon dioxide from the atmosphere. Cerium also forms cerium (III) oxide, Ce_2O_3, but CeO_2 is the most stable phase at room temperature and under atmospheric conditions.

Ceria has been used in catalytic converters in automotive applications. Since ceria can become non-stoichioimetric in oxygen content (i.e. it can give up oxygen without decomposing) depending on its ambient partial pressure of oxygen, it can release or take in oxygen in the exhaust stream of a combustion engine. In association with other catalysts, ceria can effectively reduce NO_x emissions as well as convert harmful carbon monoxide to the less harmful carbon dioxide. Ceria is particularly interesting for catalytic conversion economically because it has been

shown that adding comparatively inexpensive ceria can allow for substantial reductions in the amount of platinum needed for complete oxidation of NO_x and other harmful products of incomplete combustion.

Due to its fluorite structure, the oxygen atoms in a ceria crystal are all in a plane with one another, allowing for rapid diffusion as a function of the number of oxygen vacancies. As the number of vacancies increases, the ease at which oxygen can move around in the crystal increases, allowing the ceria to reduce and oxidize molecules or co-catalysts on its surface. It has been shown that the catalytic activity of ceria is directly related to the number of oxygen vacancies in the crystal, frequently measured by using X-Ray Photoelectron Spectroscopy to compare the ratios of Ce^{3+} to Ce^{4+} in the crystal.

Ceria can also be used as a co-catalyst in a number of reactions, including the water-gas shift and steam reforming of ethanol or diesel fuel into hydrogen gas and carbon dioxide (with varying combinations of rhodium oxide, iron oxide, cobalt oxide, nickel oxide, platinum, and gold), the Fischer-Tropsch reaction, and selected oxidation (particularly with lanthanum). In each case, it has been shown that increasing the ceria oxygen defect concentration will result in increased catalytic activity, making it very interesting as a nanocrystalline co-catalyst due to the heightened number of oxygen defects as crystallite size decreases—at very small sizes, as many as 10% of the oxygen sites in the fluorite structure crystallites will be vacancies, resulting in exceptionally high diffusion rates [12].

Table 2.1 Ceria properties [12]

Molecular formula	CeO_2
Molar mass	172.115 g/mol Appearance white or pale yellow solid,slightly
Hygroscopic Density	7.65 g/cm^3, solid 7.215 g/cm^3, fluorite phase
Melting point	2400 °C
Boiling point	3500 °C
Solubility in water	Insoluble

2.3 Nickel is a metallic chemical element, classified among the transition metals on the periodic table of elements. Humans have been using nickel in alloys for thousands of years, as traces of the metal in ancient statues and weapons indicate, although they may not have been aware of the precise properties of the element. There are a number of commercial applications for nickel, making it a very valuable and useful metal; several corporations specialize in mining and processing nickel ore, along with other metallic elements.

Pure nickel is silvery gray in appearance, and it can be polished to a bright shine. The metal is also ferromagnetic, and very ductile, meaning that it can easily be melted and worked. Nickel is relatively hard and strong, making it a great addition to alloys with softer or more fragile metals. On the periodic table of elements, it is identified with the symbol Ni, and it has an atomic number of 28 [13].

Table 2.2 Nickel properties [13]

Atomic number	28
Atomic mass	58.71 $g.mol^{-1}$
Electronegativity according to Pauling	1.8
Density	8.9 $g.cm^{-3}$ at 20°C
Melting point	1453 °C
Boiling point	2913 °C
Vanderwaals radius	0.124 nm
Ionic radius	0.069 nm (+2) ; 0.06 nm (+3)
Isotopes	10
Electronic shell	[Ar] $3d^8$ $4s^2$
Energy of first ionisation	735 $kJ.mol^{-1}$
Energy of second ionisation	1753 $kJ.mol^{-1}$
Energy of third ionisation	3387 $kJ.mol^{-1}$
Standard potential	- 0.25 V
Discovered by	Alex Constedt 1751

2.3.1 Nickel peroxide oxidizing agents

The nickel peroxide formed by treating a nickel salt with an alkali hypohalite or persulfate has been disclosed as being particularly useful for oxidizing an unsaturated alcohol to the corresponding carbonyl compound. Problems have been encountered however in preparing and using nickel peroxide oxidizing agents outside of the laboratory. Nickel peroxide oxidizing agents have been found, for example, when prepared in bulk, by treating a nickel salt with an alkali hypohalite or persulfate, to coagulate on drying into impractically large aggregates. In this regard, it has been found that the consistency and selectivity of oxidations with nickel peroxide depend to a large extent upon using a fine and uniform nickel peroxide powder. As a result, the commercial preparation of efficient and selective nickel peroxide oxidizing agents has heretofore involved costly and time consuming operations to convert the nickel peroxide aggregates, as formed, to a suitable, fine, free-flowing form.

Furthermore, large scale oxidations utilizing heretofore available nickel peroxide oxidizing agents, formed by treating nickel salts with an alkali hypohalite or persulfate, have been difficult to control. Over-oxidation of unsaturated alcohol starting materials has been a frequently encountered problem. This has resulted, for example, in the formation of relatively large amounts of acids and other by-products, rather than carbonyl compounds, from the oxidation of unsaturated alcohols. Yields have fluctuated widely and have been generally inferior to the yields obtained in the laboratory.

There has been a need therefore for an improved nickel peroxide oxidizing agent which provides consistently high yields and which does not require costly treatment to convert it to a suitably fine, free-flowing form [14].

2.4 Method of synthesis

2.4.1 Co-precipitation

Often the solubility of an element is lower in the soil solution than predicted by the solubility product because the solubility of an ion is lower in mixed ionic solution than in pure ionic solutions. One possible reason for the reduced solubility is due to co-precipitation. Co-precipitation is the incorporation of trace element into mineral structure during solid solution

formation and recrystallization of minerals. This process will reduce the mobility and toxicity of the toxic trace elements that are incorporated into the mineral.

Minerals will only incorporate elements into their structure that have similar ionic radii as the elements composing the mineral. For example, during the formation of calcite, Mn^{2+}, Cd^{2+}, and Fe^{2+} can possibly be incorporated into the mineral structure. In the formation of Fe and Al-oxides, Cr^{3+}, Mn^{3+}, and V^{3+} may be incorporated into the structure. Mn and Fe-oxides have more possibility for co-precipitation than Al-oxides and aluminosilicate minerals. Co-precipitation reactions are also controlled by the rate of soil mineral dissolution.

Precipitation reactions in soils have the ability to reduce the toxicity and mobility of harmful trace elements that may be present in the soil system. These reactions occur naturally in the soil. Surface precipitation has been used as a method of natural attenuation in marshland near San Francisco. Buried paint chips containing zinc were found in the soil at the site. It was determined that the zinc that was leaching was precipitating out of soil solution into an insoluble and immobile form. The company was permitted to put a soil cap over the contaminated area, saving them the cost of excavation and incineration. Currently, precipitation is not commonly used as a method of attenuating polluted soil. This is because there are many factors that may cause the precipitates to dissolve and again become mobile. Also, other chemical reactions are competing with precipitation in the soil and may cause the pollutant to remain soluble [15].

2.4.2 Urea hydrolysis Method

Urea has a number of properties that makes its use as an agent for precipitation from "homogeneous" solution very attractive and it has long been used in gravimetric analysis to precipitate several metal ions as hydroxides or as insoluble salts when in the presence of a suitable anion. Urea is a very weak Brønsted base (pKb = 13.8), highly soluble in water, and its hydrolysis rate may be easily controlled by controlling the temperature of the mixture. Hydrolysis of urea proceeds in two steps, the formation of ammonium cyanate (NH_4CNO) being the rate determining step, with subsequent fast hydrolysis of the cyanate to ammonium carbonate:

$$CO(NH_2)_2 \rightarrow NH_4CNO \quad (2.1)$$

$$NH_4CNO + 2H_2O \rightarrow 2NH_4^+ + CO_3^{2-} \quad (2.2)$$

The hydrolysis reactions of ammonium ions to give ammonia and carbonate to give hydrogen carbonate result in a pH of about 9, depending on the temperature. This pH is suitable for precipitating a large number of metal hydroxides [16].

2.5 Characterization of catalyst

2.5.1 Thermogravimetric analysis (TGA)

Thermo gravimetric analysis is a type of testing performed on samples that determines changes in weight in relation to change in temperature. Such analysis relies on a high degree of precision in three measurements: weight, temperature, and temperature change. As many weight loss curves look similar, the weight loss curve may require transformation before results may be interpreted. A derivative weight loss curve can identify the point where weight loss is most apparent. Again, interpretation is limited without further modifications and deconvolution of the overlapping peaks may be required.

Simultaneous TGA-DTA/DSC measures both heat flow and weight changes (TGA) in a material as a function of temperature or time in a controlled atmosphere. Simultaneous measurement of these two material properties not only improves productivity but also simplifies interpretation of the results. The complementary information obtained allows differentiation between endothermic and exothermic events with no associated weight loss (e.g., melting and crystallization) and those that involve a weight loss (e.g., degradation).

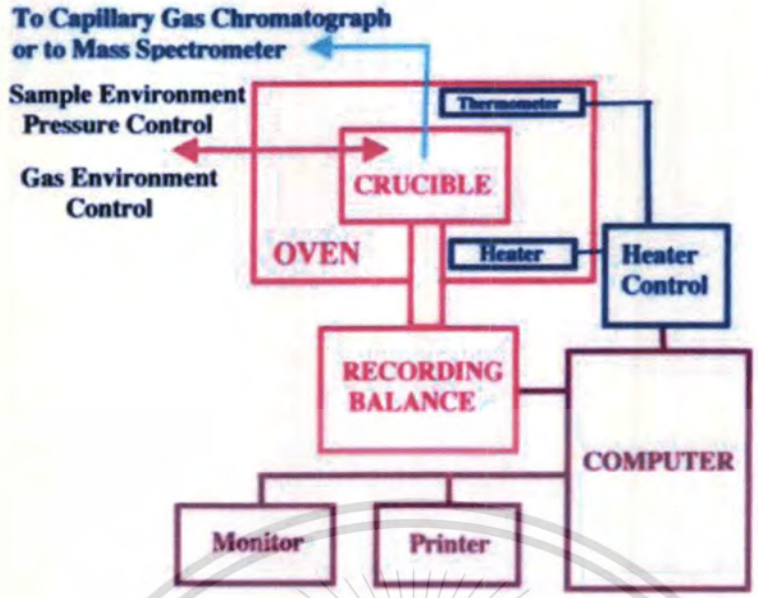

Figure 2.2 Diagram of Thermo gravimetric (TGA) [17]

TGA Thermo gravimetric Capabilities:

- Compositional analysis of materials
- Decomposition temperatures
- Rate of degradation
- Product lifetimes
- Oxidative stability
- Evaluation of polymer flam abilities
- Thermal stabilities
- Determination of rancidity of edible oils
- Fingerprinting unknown polymers
- Moisture Content
- **Volatiles content, VOC analysis**
- **Analysis of evolved gases using TGA/FTIR**
- **Competitive product evaluation**
- **Measurement of oil extender content in elastomers**
- **Effects of reactive atmospheres on materials**
- **Determination of inert filler or ash contents**

- ASTM D6375 Noack Method

Equipment

The analyzer usually consists of a high-precision balance with a pan (generally platinum) loaded with the sample. A different process using a quartz crystal microbalance has been devised for measuring smaller samples on the order of a microgram (versus milligram with conventional TGA). The sample is placed in a small electrically heated oven with a thermocouple to accurately measure the temperature. The atmosphere may be purged with an inert gas to prevent oxidation or other undesired reactions. A computer is used to control the instrument.

Methodology

Analysis is carried out by raising the temperature of the sample gradually and plotting weight (percentage) against temperature. The temperature in many testing methods routinely reaches 1000°C or greater. After the data are obtained, curve smoothing and other operations may be done to find the exact points of inflection.

A method known as hi-resolution TGA is often employed to obtain greater accuracy in areas where the derivative curve peaks. In this method, temperature increase slows as weight loss increases. This is to more accurately identify the exact temperature where a peak occurs. Several modern TGA devices can vent burn off to an infrared spectrophotometer to analyze composition [18].

2.5.2 Scanning electron microscopy (SEM)

Scanning electron microscopy (SEM) is a method for high-resolution imaging of surfaces. The SEM uses electrons for imaging, much as a light microscope uses visible light. The advantages of SEM over light microscopy include much higher magnification (>100,000X) and greater depth of field up to 100 times that of light microscopy.

Qualitative and quantitative chemical analysis information is also obtained using an energy dispersive x-ray spectrometer (EDS) with the SEM. (see separate web page for EDS analysis) The SEM generates a beam of incident electrons in an electron column above the sample chamber. The electrons are produced by a thermal emission source, such as a heated tungsten filament, or by a field emission cathode. The energy of the incident electrons can be as

low as 100 eV or as high as 30 keV depending on the evaluation objectives. The electrons are focused into a small beam by a series of electromagnetic lenses in the SEM column. Scanning coils near the end of the column direct and position the focused beam onto the sample surface. The electron beam is scanned in a raster pattern over the surface for imaging. The beam can also be focused at a single point or scanned along a line for x-ray analysis. The beam can be focused to a final probe diameter as small as about 10 Å.

Figure 2.3 SEM image of Metal Foam Structure [19]

The incident electrons cause electrons to be emitted from the sample due to elastic and inelastic scattering events within the sample's surface and near-surface material. High-energy electrons that are ejected by an elastic collision of an incident electron, typically with a sample atom's nucleus, are referred to as backscattered electrons. The energy of backscattered electrons will be comparable to that of the incident electrons. Emitted lower-energy electrons resulting from inelastic scattering are called secondary electrons. Secondary electrons can be formed by collisions with the nucleus where substantial energy loss occurs or by the ejection of loosely bound electrons from the sample atoms. The energy of secondary electrons is typically 50 eV or less.

To create an SEM image, the incident electron beam is scanned in a raster pattern across the sample's surface. The emitted electrons are detected for each position in the scanned area by an electron detector. The intensity of the emitted electron signal is displayed as brightness on a cathode ray tube (CRT). By sychromizing the CRT scan to that of the scan of the incident electron beam, the CRT display represents the morphology of the sample surface area scanned by the beam. Magnification of the CRT image is the ratio of the image display size to the sample area scanned by the electron beam.

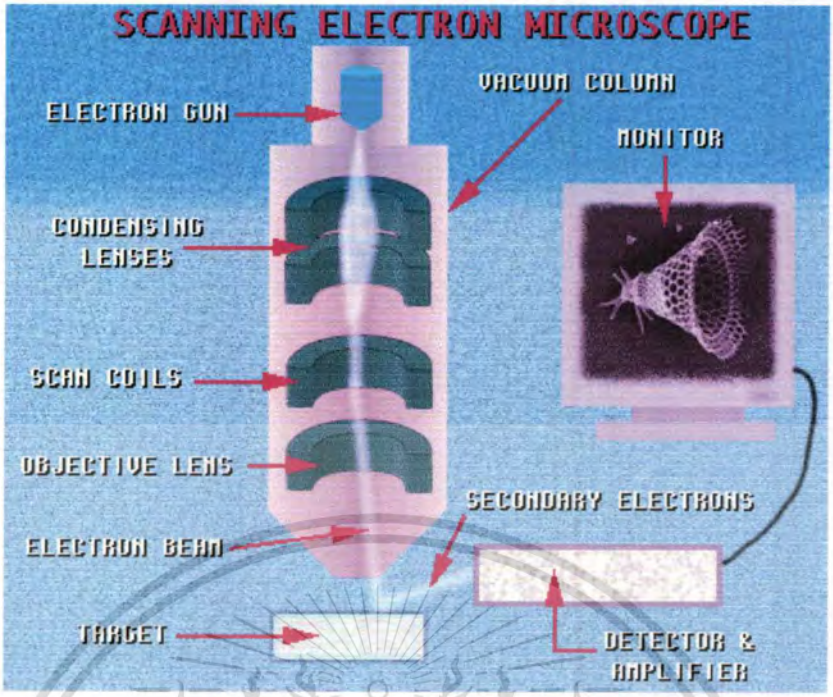

Figure 2.4 Diagram of Scanning electron microscopy (SEM)[20]

Two electron detector types are predominantly used for SEM imaging. Scintillator type detectors (Everhart-Thornley) are used for secondary electron imaging. This detector is charged with a positive voltage to attract electrons to the detector for improved signal to noise ratio. Detectors for backscattered electrons can be scintillator types or a solid-state detector.

The SEM column and sample chamber are at a moderate vacuum to allow the electrons to travel freely from the electron beam source to the sample and then to the detectors. High-resolution imaging is done with the chamber at higher vacuum, typically from 10-5 to 10-7 Torre. Imaging of nonconductive, volatile, and vacuum-sensitive samples can be performed at higher pressures.

Typical applications:

- Microscopic feature measurement
- Fracture characterization
- Microstructure studies
- Thin coating evaluations
- Surface contamination examination
- IC failure analysis

2.5.2.1 Sample Requirements

In a large-chamber SEM, samples up to 8 in. (200 mm) in diameter can be readily accommodated. Larger samples, up to 12 in. (300 mm) across can be loaded with limited stage movement. Sample height is typically limited to ~2 in. (50 mm). Backscattered electron imaging can be performed on conductive or nonconductive samples. For secondary electron imaging, samples must be electrically conductive. Nonconductive materials can be evaporatively coated with a thin film of carbon, gold or other conductive material to obtain conductivity without significantly affecting observed surface morphology

2.5.2.2 Analytical information

Secondary Electron Imaging - This mode provides high-resolution imaging of fine surface morphology. Inelastic electron scattering caused by the interaction between the sample's electrons and the incident electrons results in the emission of low-energy electrons from near the sample's surface. The topography of surface features influences the number of electrons that reach the secondary electron detector from any point on the scanned surface. This local variation in electron intensity creates the image contrast that reveals the surface morphology. The secondary electron image resolution for an ideal sample is about 3.5 nm for a tungsten-filament electron source SEM or 1.5 nm for field emission SEM.

Backscatter Electron Imaging -This mode provides image contrast as a function of elemental composition, as well as, surface topography. Backscattered electrons are produced by the elastic interactions between the sample and the incident electron beam. These high-energy electrons can escape from much deeper than secondary electrons, so surface topography is not as accurately resolved as for secondary electron imaging. The production efficiency for backscattered electrons is proportional to the sample material's mean atomic number, which results in image contrast as a function of composition, i.e., higher atomic number material appears brighter than low atomic number material in a backscattered electron image. The optimum resolution for backscattered electron imaging is about 5.5 nm.

Variable Pressure SEM - Traditionally, SEM has required an electrically-conductive sample or continuous conductive surface film to allow incident electrons to be conducted away from the

sample surface to ground. If electrons accumulate on a nonconductive surface, the charge buildup causes a divergence of the electron beam and degrades the SEM image. In variable-pressure SEM, some air is allowed into the sample chamber, and the interaction between the electron beam and the air molecules creates a cloud of positive ions around the electron beam. These ions will neutralize the negative charge from electrons collecting on the surface of a nonconductive material. SEM imaging can be performed on a nonconductive sample when the chamber pressure is maintained at a level where most of the electrons reach the sample surface, but there are enough gas molecules to ionize and neutralize charging. Variable pressure SEM is also valuable for examination of samples that are not compatible with high vacuum.

Quantization - Image magnification is calibrated against a reference standard. Lateral feature dimensions can be readily quantified to an accuracy of less than 0.1 μm. Computer analysis of images can quantify area or volume fractions and particle shapes and sizes [19].

2.5.3 X-ray Fluorescence Spectroscopy (XRF)

Although X-ray fluorescence spectroscopy is no longer regarded as a new instrumental technique for elemental analysis, ongoing evolutionary developments continue to redefine the role of this important analytical tool. From the demonstration of the first principles in the 1960's to the development of the first commercial instruments in the 1970's, the increasing availability of affordable computational power has a least been as important to the desirability and acceptance of the technology as innovative hardware design. With the widespread availability and use of a 32-bit microprocessor personal computer as the industry standard platform, X-ray fluorescence spectroscopy has become a useful and complimentary laboratory tool to other techniques.

An electron can be ejected from its atomic orbital by the absorption of a light wave (photon) of sufficient energy. The energy of the photon (hv) must be greater than the energy with which the electron is bound to the nucleus of the atom. When an inner orbital electron is ejected from an atom, an electron from a higher energy level orbital will be transferred to the lower energy level orbital. During this transition a photon maybe emitted from the atom. This fluorescent light is called the characteristic X-ray of the element. The energy of the emitted photon will be equal to the difference in energies between the two orbitals occupied by the electron making the transition. Because the energy difference between two specific orbital shells,

in a given element, is always the same (i.e. characteristic of a particular element), the photon emitted when an electron moves between these two levels, will always have the same energy. Therefore, by determining the energy (wavelength) of the X-ray light (photon) emitted by a particular element, it is possible to determine the identity of that element.

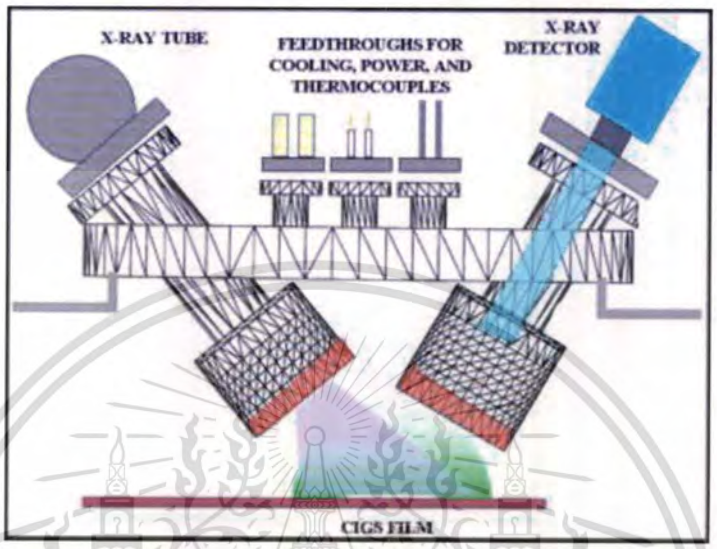

Figure 2.5 Diagram of X-ray Fluorescence Spectroscopy (XRF) [21]

For a particular energy (wavelength) of fluorescent light emitted by an element, the number of photons per unit time (generally referred to as peak intensity or count rate) is related to the amount of that analyte in the sample. The counting rates for all detectable elements within a sample are usually calculated by counting, for a set amount of time, the number of photons that are detected for the various analytes' characteristic X-ray energy lines. It is important to note that these fluorescent lines are actually observed as peaks with a semi-Gaussian distribution because of the imperfect resolution of modern detector technology. Therefore, by determining the energy of the X-ray peaks in a sample's spectrum, and by calculating the count rate of the various elemental peaks, it is possible to qualitatively establish the elemental composition of the samples and to quantitatively measure the concentration of these elements.

2.5.3.1 Introduction of sample preparation techniques for XRF analysis

X-ray fluorescence (XRF) analysis is a fast, non-destructive and environmentally friendly analysis method with very high accuracy and reproducibility. All elements of the periodic table

from beryllium to californium can be measured qualitatively, semi-quantitatively and quantitatively in powders, solids and liquids. Concentrations of up to 100% are analyzed directly, without any dilution, with reproducibilities better than ±0.1%. Typical limits of detection are from 0.1 to 10 ppm. Most modern X-ray spectrometers with modular sample changers enable fast, flexible sample handling and adaptation to customer-specific automation processes.

XRF samples can be solids such as glass, ceramic, metal, rock, coal, or plastic. They can also be liquids, like petrol, oil, paint, solutions, blood or even wine. With an XRF spectrometer both very small concentrations of very few ppm and very high concentrations of up to 100% can be analyzed directly without any dilution process. Based on its simple and fast sample preparation requirements, XRF analysis is a universal analysis method that has been widely accepted in the fields of research and industrial process control. XRF is particularly effective for complex environmental analysis and for production and quality control of intermediate and end products.

The quality of sample preparation for XRF analysis is at least as important as the quality of measurements.
An ideal sample is prepared so that it is:

- representative of the material
- homogeneous
- thick enough to meet the requirements of an infinitely thick sample
- without surface irregularities
- composed of small enough particles for the wavelengths to be measured

With XRF it is not necessary to bring solid samples into solution and then dispose of solution residues, as is the case with all wet-chemical methods. The main prerequisite for exact and reproducible analysis is a plain, homogeneous and clean analysis surface. For analysis of very light elements, e.g. beryllium, boron and carbon, the fluorescence radiation to be analyzed originates from a layer whose thickness is only a few atom layers to a few tenths of micrometer and which strongly depends on the sample. Careful sample preparation is therefore extremely important for analysis of light elements.

2.5.3.2 Preparation of Solid Samples by pressed pellets

Since powders are not affected by particle size limitations, the quickest and simplest method of sample preparation is to press the powders directly into pellets of equal density, with or without the use of a binder. In general, provided that the powder particles are less than about 50 mm in diameter, the sample will pelletize at 10 to 30 t. Where the self-binding properties of the powder are poor, higher pressure may have to be employed or in extreme cases a binder may have to be used. It is sometimes necessary to add a binder before pelletizing and the choice of the binding agent must be made with care. The binder must be free from significant contaminant elements and must have low absorption. It must also be stable under vacuum and irradiation conditions and it must not introduce significant interelement interferences. Of the large number of binding agents that have been successfully employed, probably the most useful are wax and ethyl cellulose.

The analysis of powders is invariably more complex than that of metal samples because, in addition to interelement interferences and macroscale heterogeneity, particle size effects are also important. Although inhomogeneity and particle size can often be minimized by grinding and pelletizing at high pressure, often the effects cannot be completely removed because the harder compounds present in a particular matrix are not broken down. These effects produce systematic errors in the analysis of specific type of material, such as siliceous compounds in slags, sinters and certain minerals.

Analytical data for longer wavelengths will sometimes be improved if a finely ground powder is compacted at higher pressures (say up to 30 t). A 40-ton press should be therefore considered if light element analysis is required in pressed powder samples. A good quality die set is required to produce good quality pressed powder samples. Powders can be pressed into aluminum cups or steel rings. Alternatively boric acid backing can be used, or free pressing if a binder is used [22].

2.5.4 X-ray diffraction (XRD)

The XRD technique takes a sample of the material and places a powdered sample in a holder, then the sample is illuminated with x-rays of a fixed wave-length and the intensity of the reflected radiation is recorded using a goniometer. This data is then analyzed for the reflection angle to calculate the inter-atomic spacing (D value in Angstrom units - 10^{-8} cm). The intensity (I) is measured to discriminate (using I ratios) the various D spacings and the results are to identify possible matches [23].

When the target material of the X-ray tube is bombarded with electrons accelerated from the cathode filament, two types of X-ray spectra are produced. The first is called the continuous spectra.

The continuous spectra consist of a range of wavelengths of X-rays with minimum wavelength and intensity (measured in counts per second) dependent on the target material and the voltage across the X-ray tube. The minimum wavelength decreases and the intensity increases as voltage increases.

The second type of spectra, called the characteristic spectra, is produced at high voltage as a result of specific electronic transitions that take place within individual atoms of the target material.

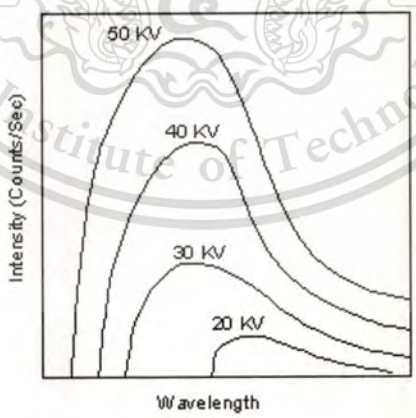

Figure 2.6 The characteristic spectra [24]

This is easiest to see using the simple Bohr model of the atom. In such a model, the nucleus of the atom containing the protons and neutrons is surrounded by shells of electrons. The innermost shell, called the K- shell, is surrounded by the L- and M - shells. When the energy of

the electrons accelerated toward the target becomes high enough to dislodge K- shell electrons, electrons from the L - and M - shells move in to take the place of those dislodged.

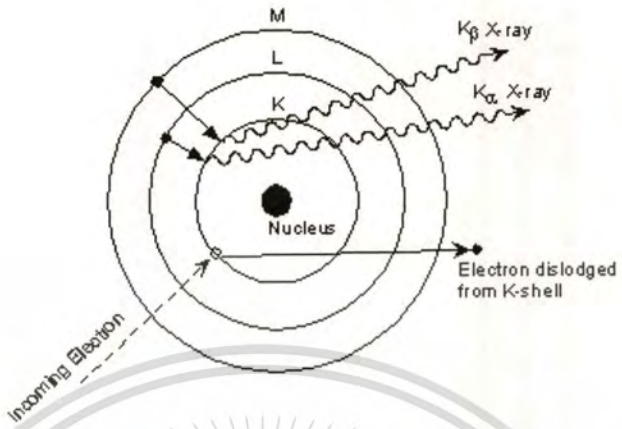

Figure 2.7 Simple Bohr model of the atom [24]

Each of these electronic transitions produces an X-ray with a wavelength that depends on the exact structure of the atom being bombarded. Transitions from the L - shell to the K- shell produces a K_a X-ray, while the transition from an M - shell to the K- shell produces a K_b X-ray.

These characteristic X-rays have a much higher intensity than those produced by the continuous spectra, with K_a X-rays having higher intensity than K_b X-rays. The important point here is that the wavelength of these characteristic x-rays is different for each atom in the periodic table (of course only those elements with higher atomic number have L- and M - shell electrons that can undergo transitions to produce X-rays). A filter is generally used to filter out the lower intensity K_b X-rays.

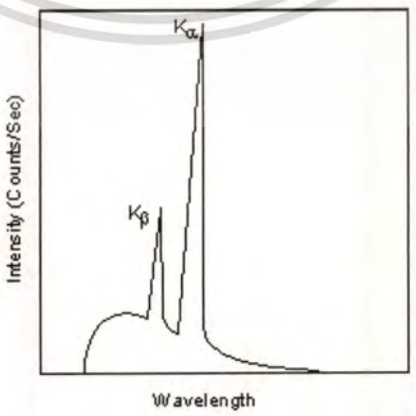

Figure 2.8 The continuous spectra of k_β and k_α [24]

2.5.4.1 X-ray Diffraction and Bragg's Law

Since a beam of X-rays consists of a bundle of separate waves, the waves can interact with one another. Such interaction is termed interference. If all the waves in the bundle are in phase, that is their crests and troughs occur at exactly the same position (the same as being an integer number of wavelengths out of phase, nl, n = 1, 2, 3, 4, etc.), the waves will interfere with one another and their amplitudes will add together to produce a resultant wave that is has a higher amplitude (the sum of all the waves that are in phase.

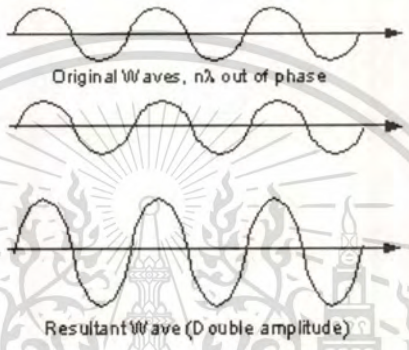

Figure 2.9 Interference termed of interaction [24]

If the waves are out of phase, being off by a non-integer number of wavelengths, then destructive interference will occur and the amplitude of the waves will be reduced. In an extreme case, if the waves are out of phase by an odd multiple of 1/2l [(2n+1)/2l], the resultant wave will have no amplitude and thus be completely destroyed.

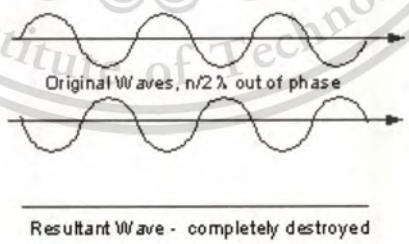

Figure 2.10 Destructive interference of interaction [24]

The atoms in crystals interact with X-ray waves in such a way as to produce interference. The interaction can be thought of as if the atoms in a crystal structure reflect the waves. But, because a crystal structure consists of an orderly arrangement of atoms, the reflections occur from what appears to be planes of atoms. Let's imagine a beam of X-rays

entering a crystal with one of these planes of atoms oriented at an angle of q to the incoming beam of monochromatic X-rays (monochromatic means one color, or in this case 1 discreet wavelength as produced by the characteristic spectra of the X-ray tube).

Two such X-rays are shown here, where the spacing between the atomic planes occurs over the distance, d. Ray 1 reflects off of the upper atomic plane at an angle θ equal to its angle of incidence. Similarly, Ray 2 reflects off the lower atomic plane at the same angle θ. While Ray 2 is in the crystal, however, it travels a distance of 2a farther than Ray 1. If this distance 2a is equal to an integral number of wavelengths (nl), then Rays 1 and 2 will be in phase on their exit from the crystal and constructive interference will occur.

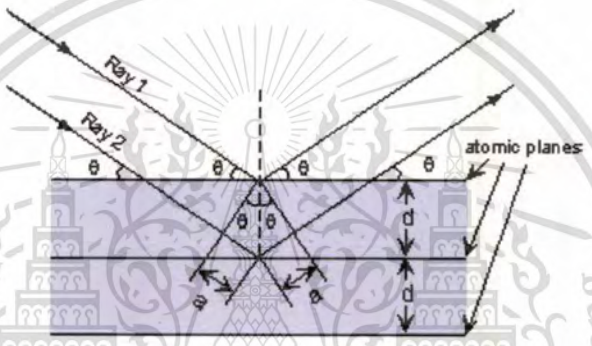

Figure 2.11 The spacing between the atomic planes [24]

If the distance 2a is not an integral number of wavelengths, then destructive interference will occur and the waves will not be as strong as when they entered the crystal. Thus, the condition for constructive interference to occur is

$$nl = 2a \tag{2.3}$$

But, from trigonometry, we can figure out what the distance 2a is in terms of the spacing, d, between the atomic planes.

$$a = d \sin \theta \tag{2.4}$$

$$\text{Or} \quad 2a = 2\, d \sin \theta \tag{2.5}$$

$$\text{Thus,} \quad nl = 2d \sin \theta \tag{2.6}$$

This is known as Bragg's Law for X-ray diffraction.

What it says is that if we know the wavelength ,l , of the X-rays going in to the crystal, and we can measure the angle θ of the diffracted X-rays coming out of the crystal, then we know the spacing (referred to as d-spacing) between the atomic planes.

$$d = nl /2 \sin \theta \quad (2.7)$$

Again it is important to point out that this diffraction will only occur if the rays are in phase when they emerge, and this will only occur at the appropriate value of n (1, 2, 3, etc.) and θ.

In theory, then we could re-orient the crystal so that another atomic plane is exposed and measure the d-spacing between all atomic planes in the crystal, eventually leading us to determine the crystal structure and the size of the unit cell [24].

2.5.4.2 X-ray Diffraction and Sherrer's equation

The Particle size of catalysts was calculated by Sherrer's equation as follows:

$$D = \frac{K\lambda}{\beta cos\theta} \quad (2.8)$$

When D = Particle size

K = Constant value which depends on size and shape of particle

β= wideness of peak that has half height of peak height (FWHM) [24]

2.5.5 Temperature Programmed Reduction (TPR)

TPR techniques permit to find the most efficient reduction conditions. Furthermore, the supported precursor phases and their interactions with the support can be identified. These experiments are particularly useful in case of multi-metallic systems, for the evaluation of the role of the added compounds or doping agents (alloy formations or promotion effects).

In the TPR technique an oxidized catalyst precursor is submitted to a programmed temperature rise, while a reducing gas mixture is flowed over it (usually, hydrogen diluted in some inert gas like argon).

The reduction rates are continuously measured by monitoring the change in composition of the reactive mixture after the reactor. The decrease in H_2 concentration in the effluent gas with respect to the initial percentage monitors the reaction progress. An interesting application of this technique is that the TPR analysis may be used to obtain evidence for the interaction between the atoms of two metallic components, in the case of bimetallic system or alloy as already cited.

In general, TPR studies are carried out under low partial pressure of the reactive gas. In this way it is possible to observe the intermediate reactions, depending from analytical conditions such as temperature rate, flow rate and concentration of reactive gas. The TPR methods are used for qualitative and quantitative analysis. In effect, the spectra produced are characteristic of a given solid [25].

The TPR method yields quantitative information of the reducibility of the oxide's surface, as well as the heterogeneity of the reducible surface. TPR is a method in which a reducing gas mixture (typically 3% to 17% hydrogen diluted in argon or nitrogen) flows over the sample. A thermal conductivity detector (TCD) is used to measure changes in the thermal conductivity of the gas stream. The TCD signal is then converted to concentration of active gas using a level calibration. Integrating the area under the concentration vs. time (or temperature) yields total gas consumed. Figure 2.12 shows a TPR profile for the reaction where M_xO_y is a metal oxide.

$$M_xO_y + yH_2 \longrightarrow xM + yH_2O \qquad (2.9)$$

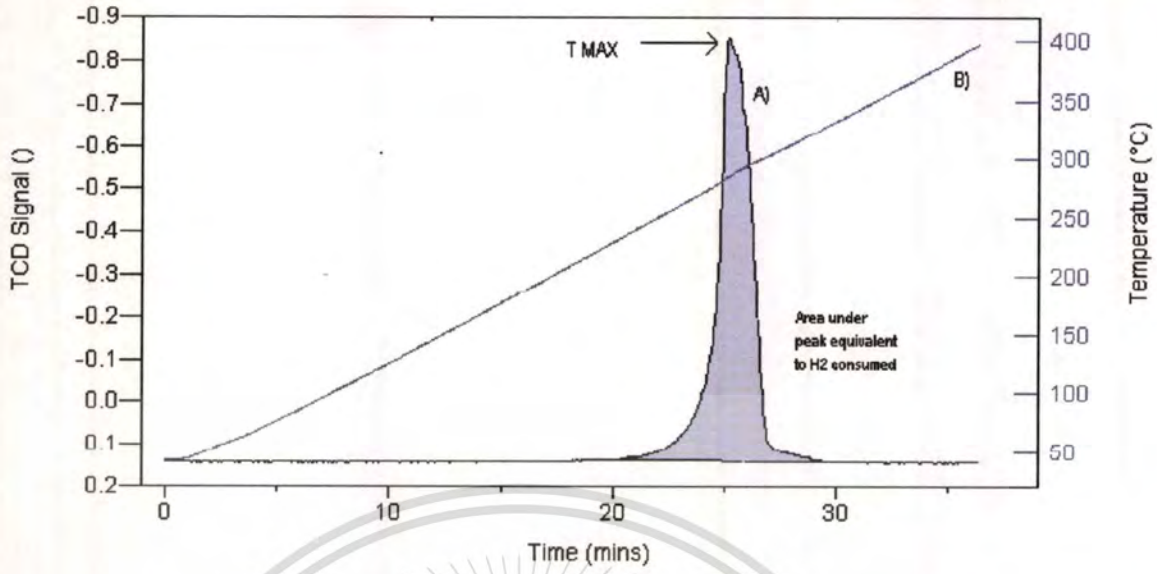

Figure 2.12. Temperature-programmed reduction profile for a metal oxide. Trace A displays the TCD signal output as a function of time. Trace B displays the temperature as a function of time during a 10 °C heating rate from ambient to 400 °C [26]

This figure illustrates a TPR spectrum where the peak maximum indicates the temperature that corresponds to the maximum rate of reduction. The TPR method provides a qualitative, and sometimes quantitative, picture of the reproducibility of the catalyst surface, as well as its high sensitivity to chemical changes resulting from promoters or metal/support interactions. Therefore, the TPR method is also suitable for quality control of different catalyst charges since deviations in manufacturing methods often result in different reduction profiles [26].

2.6 Related literature

2.6.1 Yong Li and group [27]

The catalytic behavior of Ni/CeO_2 catalysts was investigated for methane decomposition at 773 K. Ni/CeO_2 catalysts prepared by impregnation and deposition–precipitation methods showed much higher hydrogen formation rates than that of Ni/CeO_2 catalyst prepared by co-precipitation method, which exhibited relatively higher CO formation rate. CH_4-TPSR measurements confirmed that CO formation is inevitable during methane decomposition, since

the lattice oxygen of ceria could react with the deposited carbons. TEM observations further indicated that the morphologies as well as the reactivities of the deposited carbons are strongly dependent on the interaction degrees between Ni and ceria, which in turn explains the differences in the catalytic activity of the Ni/CeO_2 catalysts for methane decomposition. The Ni/CeO_2 catalyst prepared by co-precipitation method exhibited rather strong metal–support interaction probably through the formation of Ni–O–Ce solid solution, resulting in much lower hydrogen formation rate and relatively higher CO production.

2.6.2 J.A. Montoya and group [28]

Ni/ZrO_2 catalysts promoted with different amounts of CeO_2 (0, 1, 8 and 20 wt. %) were prepared by the sol–gel method. The catalysts were characterized after calcination at 800°C and after reaction of CH_4 reforming with CO_2. Rietveld analysis reveals that the tetragonal ZrO_2 phase (t-ZrO_2) present in the catalysts is stabilized by the CeO_2, forming a solid solution, and avoiding transformation to the monoclinic phase (m-ZrO_2). Ni_2C also competes with Ce_4C in the incorporation to t-ZrO_2. The t-ZrO_2 stability increases with CeO_2 concentration. The catalyst activity is increased with the CeO_2content, although some degree of deactivation, due mainly to the sintering of the support, was not completely avoided by ceria addition. The deposition of graphitic carbon does not play an important role in the catalysts deactivation. The catalytic performance is related to the Ni surface dispersion and NiO reducibility, both promoted by CeO_2 incorporation. CeO_2 enhances the reverse water-gas shift reaction during dry reforming of methane over the studied catalysts.

2.6.3 Leung P. Tangand group [29]

Hydrogen storage and emission from Ni/Ce (0.1:1) composite oxides, prepared by the co-precipitation method at -2 °C, 22 °C and 60°C using tri-ethylamine as the precipitating agent, are investigated. The as-prepared uncalcined materials exhibit small amounts of H_2emission even without prior exposure to H_2, with the amount dependent on the synthesis temperature. Examination of the CO, CO_2 and H_2O emission profiles suggest a link between the presence and stability of carbonate species within these composite materials and the H_2 emission. Following

activation in pure hydrogen at 250 °C, all samples show increased H_2 emission levels but it is only in the sample synthesized at 60°C that a simultaneous decrease in the H_2 emission temperature is found. H_2O emission below 250 °C in the activated material indicates that this also originates from hydrogen stored in the material. The activation conditions are shown to have a significant impact on the level of H_2interaction with these materials. A marked increase of the crystallite size with synthesis temperature, from 1.7 nm at -2 °C to 11.7 nm at 60 °C, is also found. The difference in of H_2 interaction is associated with a change in the nature/morphology of the materials precipitated at the different temperatures.

2.6.4 Sitthiphong Pengpanich and group [30]

In this study, methane partial oxidation (MPO) to synthesis gas over Ni/$Ce_{1-x}Zr_xO_2$ (x = 0, 0.25, and 1.0 with varying Ni loading of 5,10 and 15 wt.%) was investigated over the temperature range of 400–800 °C. The experimental results showed that the catalysts prepared by impregnation method are more active than those prepared by gel impregnation method because of their higher degrees of metal dispersion and reducibility. Under the reaction conditions, MPO over Ni/CeO_2 and Ni/$Ce_{0.75}Zr_{0.25}O_2$ mixed oxide catalysts were active at temperatures above 550 °C whereas that of Ni/ZrO_2 took place at temperatures above 650 °C. The H_2/CO molar ratio of 2.0±0.05 was obtained. Generally, the CH_4conversion slightly increased while the CO and H_2 selectivities remained unchanged with increasing Ni loading. The Ni/$Ce_{0.75}Zr_{0.25}O_2$ mixed oxide catalysts were found to resist to coke formation more than the other catalysts due to their high degrees of metal dispersion and surface oxygen mobility. The TPO results indicated that a major source of carbon deposition on these catalysts is due to the methane decomposition. Results also showed that the activity and selectivity of the catalysts can be regained after the regeneration under oxidizing atmosphere.

2.6.5 Tianli Zhu and group [31]

The partial oxidation of methane to syngas was studied in this work over Ni – containing ceria catalysts with nickel content of 5, 10 and 20 at.% at atmospheric pressure. All catalysts, in the as prepared state, showed similar activity and CO selectivity at T $\geq$ 550 °C. Catalyst pre – reduction was not required. Reaction mixtures were dilute, containing 3 mol% CH_4 and 1.5 mol% O_2. Methane conversion and CO selectivity approached their respective thermodynamic

equilibrium values above 550 °C. The H_2/CO ratio was equal to 2 at T > 600 °C. In the range 0.54 – 0.04 g s/cm^3 (STP), contact time effects were absent in partial oxidation of methane over the 5 at.% Ni – Ce(La)O_x catalyst. The phase composition, nickel dispersion and carbon deposition on the catalysts were investigated by various characterization techniques, including XRD, STEM/EDS, XPS and TPO analyses. The 5 at.% Ni – Ce(La)O_x catalyst, comprising highly dispersed nickel oxide in ceria, showed excellent resistance to carbon deposition and stable performance during 100 h-on-stream at 650 °C. On the other hand, high content ($\geq$ 10 at.%) nickel in ceria, comprising both dispersed nickel and bulk nickel oxide particles, was unstable even after a much shorter time-on-stream; carbon deposition was clearly the cause of this performance instability.

2.6.6 Maria D. Salazar – Villalpando and Bryan Reyes [32]

The catalytic performance of Ni dispersed on ceria-doped supports, $(Ce_{0.88}La_{0.12})O_{2-x}$, $(Ce_{0.91}Gd_{0.09})O_{2-x}$, $(Ce_{0.71}Gd_{0.29})O_{2-x}$, $(Ce_{0.56}Zr_{0.44})O_{2-x}$ and pure ceria, was tested for the catalytic partial oxidation of Methane (CPOX). The catalysts were characterized by Brunauer Emmett Teller (BET), X-ray diffraction (XRD), temperature programmed reduction (TPR) and temperature programmed oxidation (TPO). Ni/$(Ce_{0.56}Zr_{0.44})O_{2-x}$ showed higher hydrogen production than the Ni/Gadolinium-doped catalysts, which may be due to its higher reducibility and surface area. By enhancing the support reducibility in Ni/doped-ceria catalysts, their catalytic activity is promoted because the availability of surface lattice oxygen is increased, which can participate in the formation of CO and H_2. It was also found that Ni/$(Ce_{0.56}Zr_{0.44})O_{2-x}$ showed higher catalytic performance after redox pretreatments. Similarly, a higher amount of H_2 or O_2 was consumed during hydrogenation and oxidation pretreatments, respectively. This may be correlated to re-dispersion of metallic particles and changes on the metal-support interface. In addition, it was observed that the ionic conductivity of Ni/$(Ce_{0.56}Zr_{0.44})O_{2-x}$ had an effect on the amount of carbon formed during the CPOX reaction at oxygen concentrations lower than the stoichiometric required, O/C ratios lower than 0.6. Its high oxygen mobility may have accelerated the surface

oxidation reactions of carbon by reactive oxygen species, thus, inhibiting carbon growth on the catalyst surface.

2.6.7 Meiling Teng and group [33]

Mesoporous $Ce_{1-x}Zr_xO_2$ (m-$Ce_{1-x}Zr_xO_2$, x = 0.2 – 0.5) mixed oxide were synthesized by using polyol method. The influences of coefficient x on permanances of m-$Ce_{1-x}Zr_xO_2$ and Cu based catalyst towards CO selective oxidation in H_2-rich gas were investigated. The samples were characterized by means of XRD, Raman, FT-IR, TG, BET, Tem, TPR and TPD techniques. The results showed that all m-$Ce_{1-x}Zr_xO_2$ samples were mesoporous materials with cubic fluorite structure, and the highest surface area (181 $m^2 g^{-1}$) was obtained when the x = 0.5. Compared with CuO/m-$Ce_{1-x}Zr_xO_2$ (x = 0.2 – 0.35) catalysts, the CuO/m-$Ce_{0.5}Zr_{0.5}O_2$ catalyst had higher CO conversion and selectivity in H_2-rich gas, they were 100% and 96.2% at 383 K, respectively. This is explained in terms of its stronger interaction between active ingredient and support, higher dispersion, more active sites, larger CO adsorption amount and lower desorption temperature, which were advantageous to enhance its catalytic activity.

2.6.8 Navadol Laosiripojana and group [34]

In the present work, the catalytic cracking of methane, methanol, and ethanol with ceria (CeO_2) was investigated sing temperature-programmed reaction (TPRx) and isothermal reaction at 900 °C. Ceria showed a reasonable activity in conversion of hydrocarbon to hydrogen, carbon monoxide, and carbon dioxide with only small amounts of carbon deposition observed compared to conventional Ni/Al_2O_3 even though the methanol and ethanol were fed. In addition, from the catalytic cracking of methanol and ethanol using ceria, hydrogen can be produced continuously without any requirement of oxidants due to the oxygen storage capacity of CeO_2. Oxygen atom from methanol and ethanol can oxidize the reduced state of ceria, CeO_{2-x}, from the cracking reaction and recover the oxidized state of ceria, CeO_2. However, the catalytic cracking reactivity of CeO_2 remains too low due to its low specific surface area. The use of synthesized high surface area CeO_2 improves the performance of ceria toward this reaction. The catalytic cracking of

hydrocarbon elements by high surface area CeO_2 will be studied and presented in our next publication.

2.6.9 D. Srinivas and group [35]

The influence of Ce/Zr ratio on the redox behavior of Ni in a series of $NiO-CeO_2-ZrO_2$ catalysts was investigated using in situ electron paramagnetic resonance (EPR), diffuse reflectance UV-visible (DRUV-visible) and X-ray photoelectron spectroscopy (XPS). At all concentrations, a small amount of Ni (species I) substitutes in the fluorite lattice. Superparamagnetic, nanosize Ni crystallites (species II) were found in samples with 1-5 wy.%NiO and ferromagnetic, larger Ni crystallites (species III) were detected in samples with 20 wt.% or more NiO when contacted with hydrogen. Ce promoted the reduction of Ni. The reducibility of Ni decreased in the order: I > III > II. At steam reforming conditions (in the presence of $H_2 + H_2O$ + hydrocarbon/alcohol at 773 K), the extent of Ni reduction varies in the order: H_2 + alkane > H_2 + alcohol > H_2 alone. Catalytic activity and especially stability in the steam reforming of bio-ethanol (containing 5 ppm S) correlates with the type III Ni species and is influenced by both the Ni-content and the Ce/Zr ratio in the support. A catalyst of composition NiO (40 wt.%)-CeO_2 (30 wt.%)-ZrO_2 (30 wt.%) maintained its activity for more than 500 h without deactivation.

2.6.10 Sittiphong Pengpanich and group [36]

In this study, $CeO_2 - ZrO_2$ mixed oxide catalysts were prepared via urea hydrolysis and tested for methane oxidation. Highly uniform solid solution particles of ceria – zirconia were obtained under the conditions of this study. The incorporation of Zr into the CeO_2 lattice was found to promote the redox properties. The methane oxidation activity of the mixed oxide was found to be independent on the Ce:Zr ratio, which relates to the degree of reducibility. It was postulated that the cubic phase, fluorite structure, which is mainly found in $Ce_{1-x}Zr_xO_2$ (where $x < 0.5$) can be reduced more easily than the tetragonal phase found in $Ce_{1-x}Zr_xO_2$ (where $x > 0.5$). The catalytic activity decreased with an increasing Zr content. The mixed oxide catalyst, $Ce_{0.75}Zr_{0.25}O_2$ solid solution, was reported to exhibit the highest activity for methane oxidation.

Kinetic studies of methane oxidation over such a mixed oxide catalyst ($Ce_{0.75}Zr_{0.25}O_2$) showed that the methane oxidation rates strongly depend on methane concentration, but only slightly on the oxygen concentrations. The Langmuir – Hinshelwood mechanism (oxygen dissociative chemisorptions on the active sites and non-dissociative chemisorptions of methane) can satisfactorily fit the experimental results obtained from the kinetic studies for this catalyst. The activation energy of methane oxidation is calculated based on this surface reaction mechanism as being 100.8 kJ/mol.

Chapter 3

Experimental details

3.1 Instruments and apparatus

1) Thermogravimetric analysis (TGA), series TGA Pyris I by Perkin Elmer, American

2) Scanning electron microscope (SEM), series S 3400N by Hitachi, Japan

3) X-ray fluorescence spectrometer (XRF), Philips model PW 2400, Netherland

4) X-ray diffractometer (XRD), series D8 Advance by Bruker-AXS, Germany

5) H_2-Temperature programmed reduction (H_2-TPR), series Micromeritics by Auto chem II

6) 150 ml -Beaker

7) 1000 ml - Beaker

8) Stirring rod

9) Crucible

10) Spatulas

11)150 mL -Buret

12) 500 mL - Duran® Laboratory Bottle

13) Whatman® Filtered-paper No.2

14) Filtration machine EYEL4 Aspirator A-35

15) Furnace Thermolyne 6000 muffle

16) Oven Memmer tUFB 500

17) Centrifuge CENTAUR2® MSE Sanyo

18) pH meter

3.2 Chemicals

1) Cerium (III) Nitrate 6-hydrate [$Ce(NO_3)_3 \cdot 6H_2O$]Puris grade Produced by Merck KGaA Germany

2) Nickel (II) Nitrate 6-hydrate [$Ni(NO_3)_2 \cdot 6H_2O$] Analytical Grade Produced by Sigma-Aldrich America

3) Distilled water

4) Urea palle Analytical Grade Produced by Carlo Erba, Italy

5) Ethanol (C_2H_5OH) Analytical Grade Produced by Lab-scan, Ireland

6) Sodium hydroxide anhydrous (NaOH) Analytical Grade Carlo Produced by Erba, Italy

3.3 Procedure

3.3.1 Synthesis of $Ce_{1-x}Ni_xO_2$ mixed oxide catalyst by urea hydrolysis method

1. Mixed the metal salt solution to the concentration of 0.1 M for 250 ml into 500 ml beaker. The details are shown in the Table 3-1.

2. Add 250 ml of 0.4 M urea solution to make a salt solution to urea solution ratio of 2:1 v/v.

3. Keep the mixture at 100 °C for 50 hours.

4. Cool the mixture to room temperature prior to be centrifuged.

5. Filter the gel product and wash several times with ethanol.

6. Dry in an oven at 110 °C overnight.

7. Calcine at 550 °C for 6 hours.

8. Do the same experiment for x = 0.75, $Ce_{0.25}Ni_{0.75}O_2$

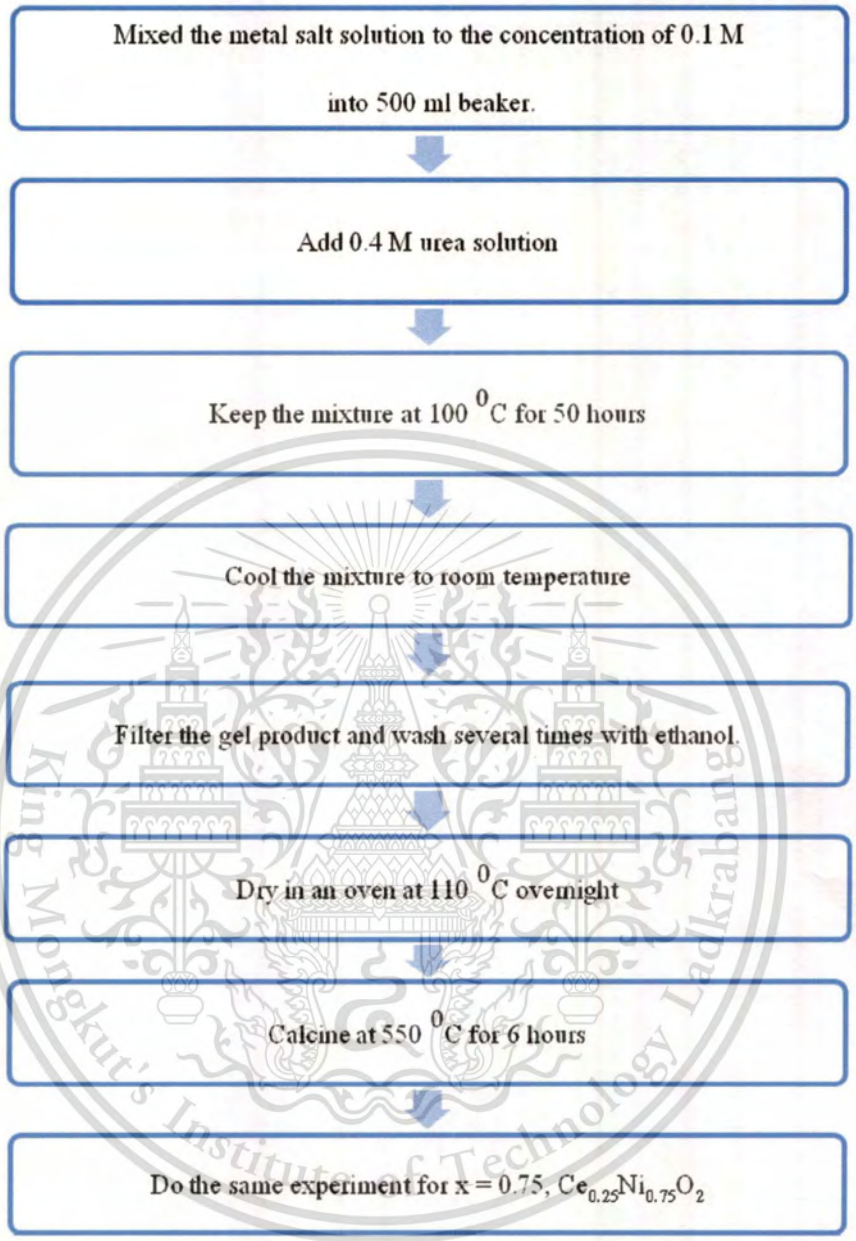

Figure 3.1 The preparation via the urea hydrolysis method.

3.3.2 Synthesis of $Ce_{1-x}Ni_xO_2$ mixed oxide catalyst by co-precipitation method

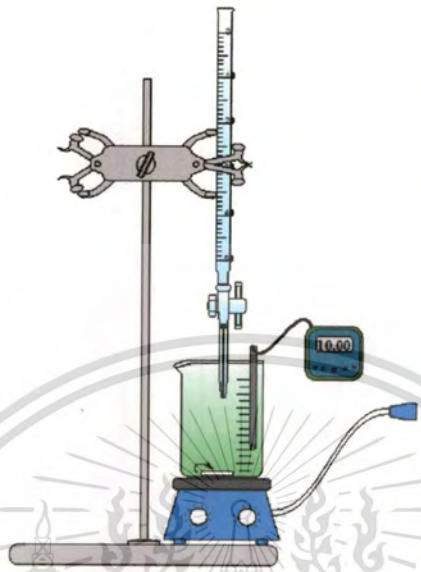

Figure 3.2 Tool set up of the co-precipitation method

1. Mixed the metal salt solution to the concentration of 0.1 M into 1000 ml beaker. The details are shown in the Table 3-2.

2. Add 0.1 M NaOH aqueous solution drop-wise into the metal - salt mixture at room temperature to reach pH of 10 and age for 48 hours.

3. Filter the mixture to obtain a precipitate.

4. Wash the precipitate several times with distilled water.

5. Dry at 110 °C overnight.

6. Calcine at 550 °C for 6 hours.

7. Do the same experiment for n = 0.75, $Ce_{0.25}Ni_{0.75}O_2$

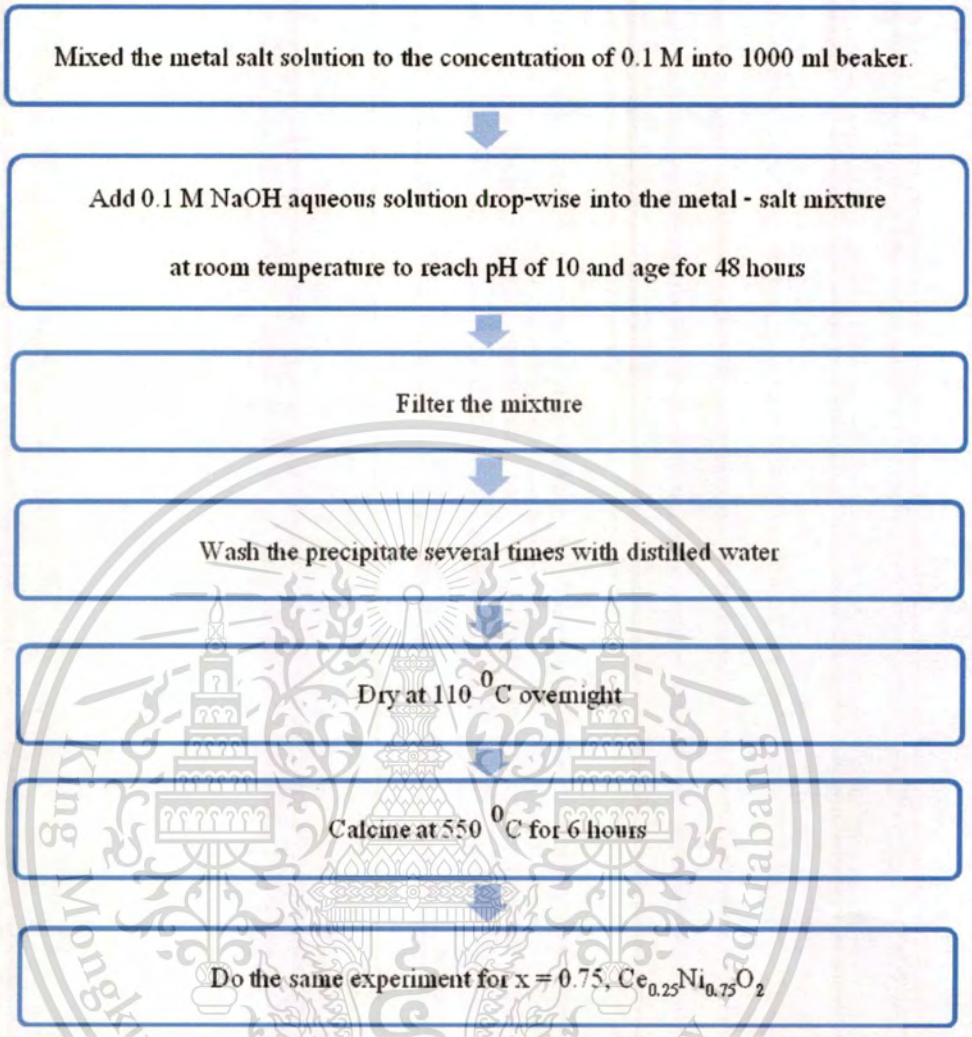

Figure 3.3 The preparation via the co-precipitate method.

Table 3.1 The composition of metal salt solutions for the urea hydrolysis method.

x	0.1M $Ce(NO_3)_3 \cdot 6H_2O$ solution		0.1M $Ni(NO_3)_2 \cdot 6H_2O$ solution		0.4M urea solution $(NH_2)_2CO$		Weight of $Ce_{1-x}Ni_xO_2$ (g)
	Weight of $Ce(NO_3)_3 \cdot 6H_2O$ (g)	Volume of distilled water (ml)	Weight of $Ni(NO_3)_2 \cdot 6H_2O$ (g)	Volume of distilled water (ml)	Weight of $(NH_2)_2CO$ (g)	Volume of distilled water (ml)	
0.25	5.2122	120	1.1624	40	1.9208	80	2.3443
	5.2106	120	1.1631	40	1.9216	80	4.3033
	5.2108	120	1.1637	40	1.9216	80	
0.75	1.7319	40	3.4891	120	1.9231	80	1.9327
	1.7366	40	3.4900	120	1.9221	80	3.0906
	1.7371	40	3.4898	120	1.9216	80	

Table 3.2 The composition of metal salt solutions for the co-precipitation method.

x	0.1M $Ce(NO_3)_3 \cdot 6H_2O$ solution		0.1M $Ni(NO_3)_2 \cdot 6H_2O$ solution		0.1M NaOH solution		Weight of $Ce_{1-x}Ni_xO_2$ (g)
	Weight of $Ce(NO_3)_3 \cdot 6H_2O$ (g)	Volume of distilled water (ml)	Weight of $Ni(NO_3)_2 \cdot 6H_2O$ (g)	Volume of distilled water (ml)	Weight of NaOH (g)	Volume of distilled water (ml)	
0.25	6.5123	150	1.4576	50	3.9475	1000	2.8003
	13.0285	300	2.9022	100			5.6202
0.75	2.8962	67	5.8151	200	3.9521		2.5214
	5.7897	134	11.6312	400	3.9759		5.1241

3.3.3 Characterization of the mixed oxide solid solutions

1. Thermogravimetric analysis (TGA)

- It is used to determine changes in weight in relation to change in temperature.

- The 0.02 g of sample was placed on high-precision balance; a pen.

- A quartz crystal microbalance has been devised for measuring smaller samples on the order of a microgram.

- The pen was placed in a small electrically heated oven with a thermocouple to accurately measure the temperature.

- The inert gas; N_2 gas was purged with the heating rate of 20 °C/min.

- The computer was used to control the instrument.

2. Scanning electron microscope (SEM)

- It is used to observe the morphology of the catalysts.

- The electron gun of SEM generates a beam of incident electrons in an electron column above the sample chamber.

- Scanning coils focus a beam onto the sample surface.

- The electron beam is scanned in a raster pattern over the surface for imaging.

- The emitted electrons are detected for each position in the scanned area by an electron detector, the CRT display represents the morphology of the sample surface area scanned by the beam.

3. X-ray fluorescence (XRF)

- It is used to identify, and sometimes quantify, elements present in a material by measuring the emission of X-ray fluorescence from a material that has been excited by bombarding with high-energy X-ray.

- Mixed the samples with boric acid in 1:3 ratio, then compressed at 150 kN into the pellet.

4. X-ray diffractometer (XRD)

- It is used to identify the different phases in the catalyst as well as examine its crystalline structure by using Cu K_α radiation.

- The intensity data were collected at 25 °C over a 2θ range of 20 -80 °C with a scan speed of 5° (2θ)/ min and a scan step of 0.02° (2θ).

5. H_2-Temperature programmed reduction (H_2-TPR)

- It is used to study the reducibility of NiO after calcination.

- The sample was pretreated in Ar atmosphere at 400 °C for 30 minutes prior to running the TPR experiment.

- Then the sample was cooled down to room temperature in ambient Ar.

- A 5% H_2/Ar gas was used as a reducing gas.

- The sample temperature was raised at a constant rate of 10 °C min^{-1} from room temperature to 700 °C.

- The amount of H_2 consumption as a function of temperature was determined from a TCD signal.

Chapter 4

Results and Discussion

This research tried to synthesize and characterize the Ni/CeO_2 catalysts ($Ce_{1-x}Ni_xO_2$) in the different mole ratio (x = 0.25, and 0.75) and preparation methods. Two methods were used to prepare the catalysts, the co – precipitation method and the urea hydrolysis method. The characterization methods included TGA, SEM, XRF, XRD, and H_2-TPR.

The results were discussed in the term of the comparison of the catalysts in the different mole ratio with the same preparation method and in the different preparation method with the same mole ratio.

4.1 The characterization by the Thermogravimetric analysis (TGA)

The study of the decomposition when the catalysts were heated by the thermogravimetric analysis explains the information of the thermal decomposition in the reaction and the change of the catalysts structures. Ar gas was purged with the heating rate of 20 °C/min to determine the chemical compositions which lost the weights by thermal decomposition. This information is used to designate the temperature range that was suitable for the calcinations of the $Ce_{1-x}Ni_xO_2$ mixed oxide catalysts.

Table 4.1 The temperature ranges and the percent of weight loss of the $Ce_{1-x}Ni_xO_2$ mixed oxide catalysts before calcination.

Sample		Temperature range of thermal decomposition (°C)			Weight loss (%)		
		1st range	2nd range	3rd range	1st range	2nd range	3rd range
Co-precipitation method	X = 0.25	35-225	226-330	331-421	7.58	2.87	3.66
	X = 0.75	38-222	223-345	-	6.13	13.49	-
Urea Hydrolysis method	X = 0.25	141-440	-	-	28.05	-	-
	X = 0.75	30-379	380-480	-	24.34	9.70	-

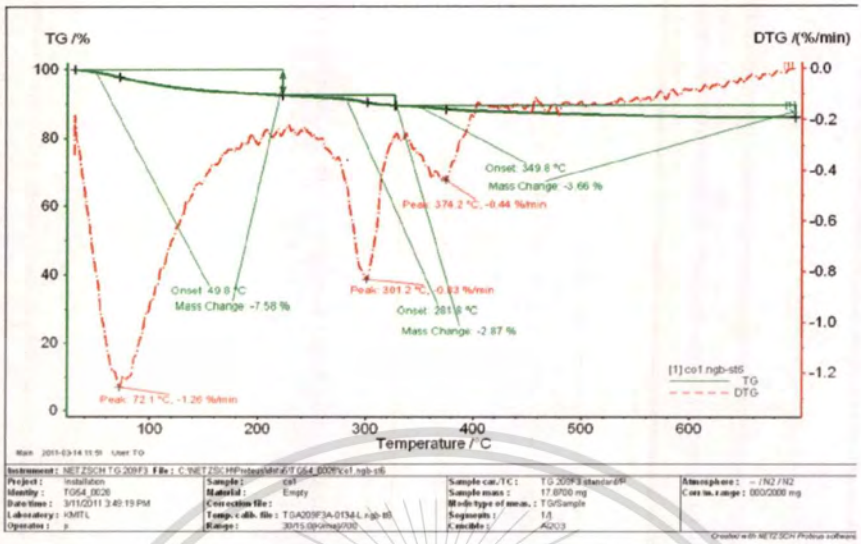

Figure 4.1 (a) The TGA/DTG diagram of the $Ce_{1-x}Ni_xO_2$ catalyst prepared via the co – precipitation method when x = 0.25

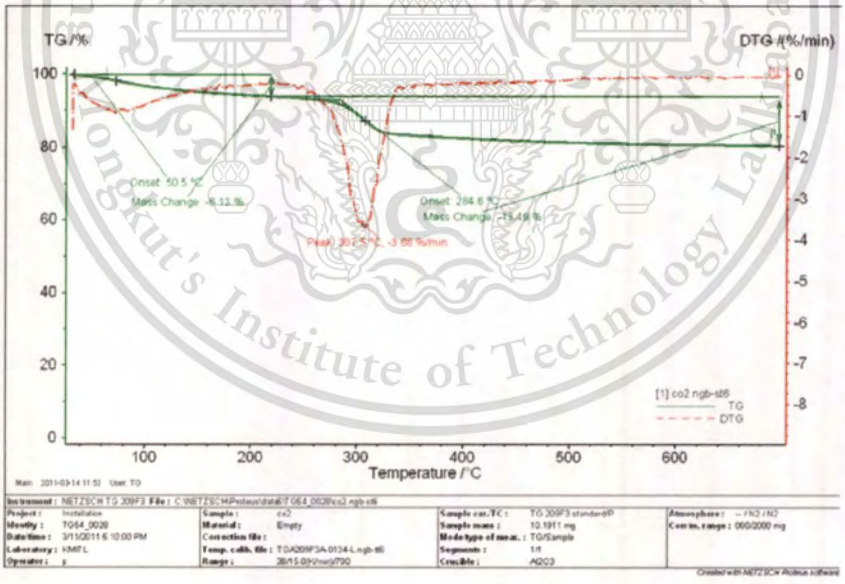

Figure 4.1 (b) The TGA/DTG diagram of the $Ce_{1-x}Ni_xO_2$ catalyst prepared via the co – precipitation method when x = 0.75

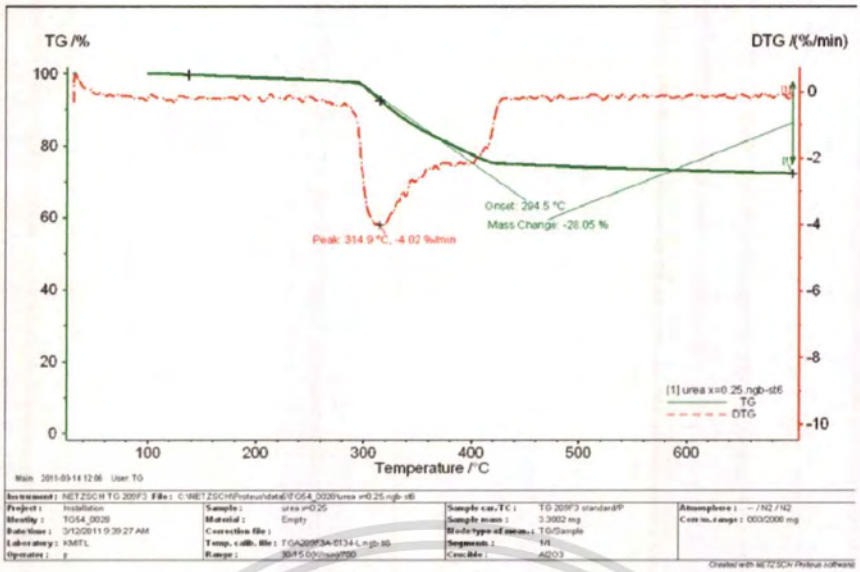

Figure 4.1 (c) The TGA/DTG diagram of the $Ce_{1-x}Ni_xO_2$ catalyst prepared via the urea hydrolysis method when x = 0.25

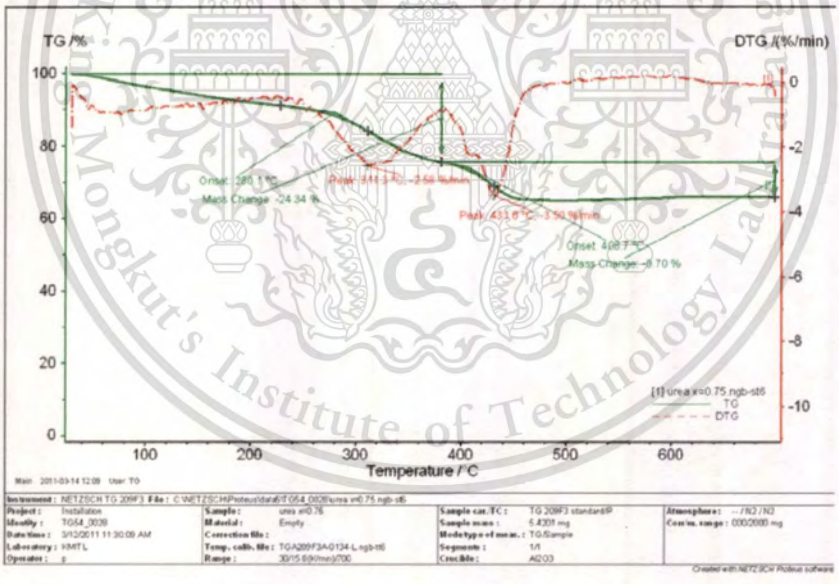

Figure 4.1 (d) The TGA/DTG diagram of the $Ce_{1-x}Ni_xO_2$ catalyst prepared via the urea hydrolysis method when x = 0.75

The figure 4.1 showed the diagram of the $Ce_{1-x}Ni_xO_2$ mixed oxide catalysts prepared via co – precipitation and urea hydrolysis methods, respectively, when molar ratios were equal to 0.25 (x = 0.25) and 0.75 (x=0.75).

For the $Ce_{0.75}Ni_{0.25}O_2$ mixed oxide catalysts prepared via co-precipitation method; it was found that there was the weight loss and thermal change in three stages. The first stage, at the temperature range of 35-225°C, the weight loss was 7.58% indicated that it was due to the removal of water molecules. The second stage, at the temperature range of 226-330°C, the weight loss was 2.87% due to the removal of some elements. From reactants, it should be the NO_3^{2-}. And the third stage, at the temperature range of 330-421°C, 3.66% was the weight loss of this peak owing to the loss of others metal. From XRF result, it might be postulated that metal was Sio_2. For the $Ce_{0.25}Ni_{0.75}O_2$ mixed oxide catalysts prepared via co-precipitation method, the weight loss was shown in two stages. The first peak of weight loss was shown between the temperature range of 38-222°C, the weight loss was 6.13% because of the removal of water molecules. And the second peak of weight loss was shown at the temperature range of 223-345°C.This was due to the thermal decomposition of some elemental compositions; it should be the NO_3^{2-} causing the weight loss to be 13.49%.

The TGA result of $Ce_{0.75}Ni_{0.25}O_2$ catalysts by urea hydrolysis method was shown in only one stage. The weight loss was 28.05% at the temperature range of 141 - 440°C due to some elemental compositions were decomposed. From reactants, it should be the NO_3^{2-}.

For the $Ce_{0.25}Ni_{0.75}O_2$ mixed oxide catalysts prepared via urea hydrolysis method, the thermal decomposition was divided into two stages. The first stage was shown between 30-379°C of temperature range for 24.34% of the weight loss because of the removal of water molecules. The 380-480°C of temperature range was shown as the second stage; the weight loss was 9.70% due to the thermal decomposition of some elemental compositions. It should be the NO_3^{2-} from reactants.

Actually, the first stage should be the removal of moisture. The thermal decomposition of some elemental compositions; it was the NO_3^{2-} should be shown in the second stage and the last stage should be the thermal decomposition of the others metal as SiO_2.

For the temperature over 550 °C, there was no weight loss shown in all diagrams. It was postulated that this temperature might be the lowest temperature for the calcinations of the

$Ce_{1-x}Ni_xO_2$ mixed oxide catalysts. Hence, the temperature of 550 °C was chosen for this experiment for further observation.

4.2 The characterization by the scanning electron microscope (SEM)

These SEM images showed the different of the catalyst's surface topography. The catalysts prepared via both preparation methods the presence of small particles, well formed and defined which present a higher contrast were observed. These images have been confirmed by using the SEM images that corresponded to the mix oxide catalyst.

4.2.1 The comparison of the catalysts with the different preparation methods.

These following images (Figs. 4.2 and 4.3) showed the different of the catalyst's surface topography between the different mole ratio and the preparation methods. For the catalysts prepared via the co-precipitation method were in the flake shapes, while via the urea hydrolysis method were in the needle shapes.

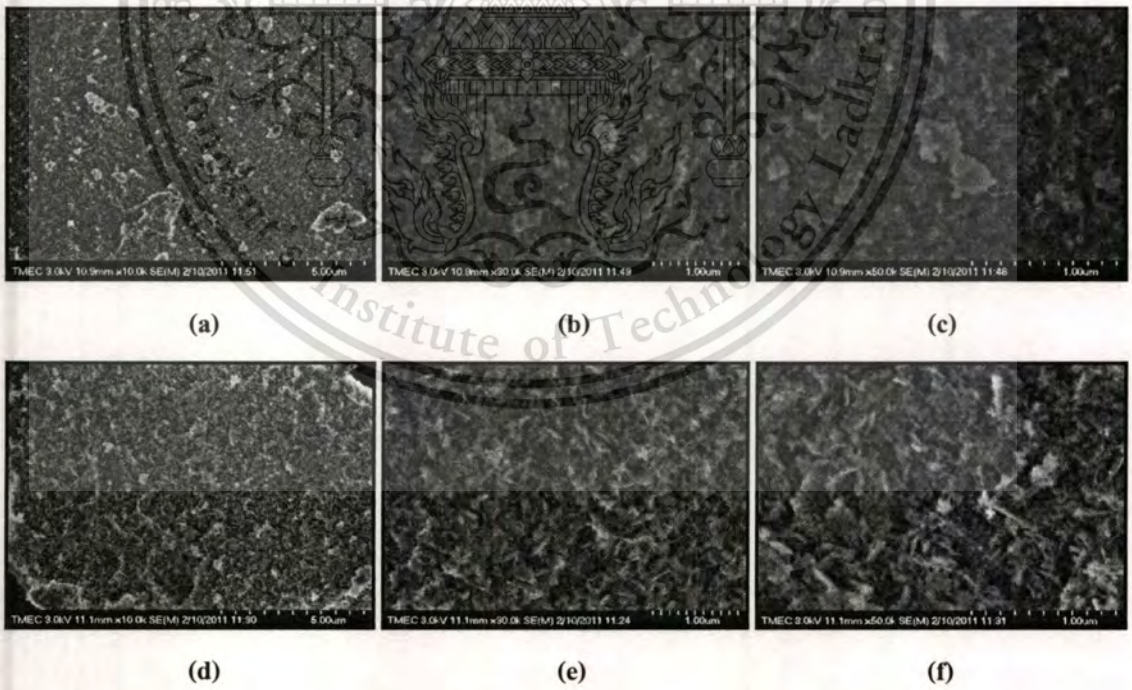

Figure 4.2 SEM images of $Ce_{1-x}Ni_xO_2$ catalysts after the calcinations at 550 °C.

Above, via co-precipitation method when x = 0.25 (a) at 10.0 k (b) at 30.0 k and (c) at 50.0k.

Below, via co-precipitation method when x = 0.75 (a) at 10.0 k (b) at 30.0 k and (c) at 50.0k.

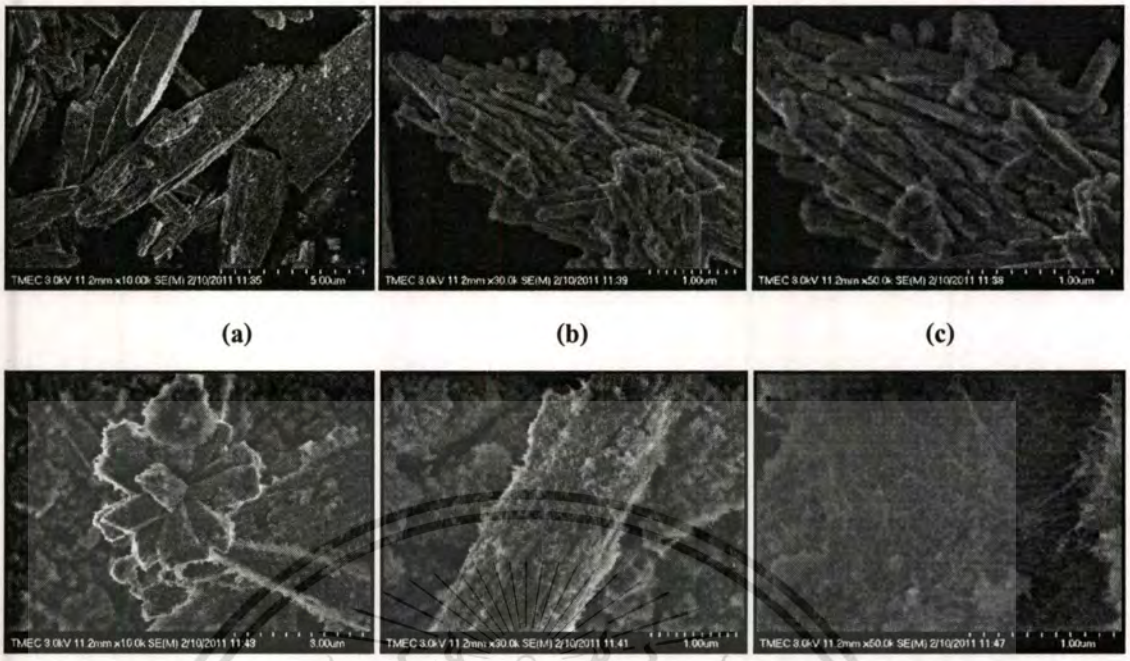

Figure 4.3 SEM images of $Ce_{1-x}Ni_xO_2$ catalysts after the calcinations at 550 °C.
Above, via urea hydrolysis method when x = 0.25 (a) at 10.0 k (b) at 30.0 k and (c) at 50.0k.
Below, via urea hydrolysis method when x = 0.75 (a) at 10.0 k (b) at 30.0 k and (c) at 50.0k.

But the difference in the preparation method clearly suggested that it was an important factor in the occurrence of the catalyst type. For catalysts prepared via co-precipitate method were observed amorphous structure, and for catalysts prepared via urea hydrolysis method were observed crystalline structure.

4.2.2 The comparison of the catalysts with the different mole ratio

In the same preparation method, the difference in mole ratio (x = 0.25 and 0.75) revealed only a little change of the catalysts shape, but in Figs. 4.2 and Fig. 4.3 indicated that the mole ratio had a significant effect on the properties of the catalysts. Urea hydrolysis catalyst with molar ratio x=0.25 were occur as mix oxide solid solution while catalysts with molar ratio x=0.75 occur as NiO/CeO. The differences were somehow enhanced in the case of ceria (CeO_2) which was used as the supporter enabled a high degree of homogeneity to be achieved, or NiO in catalyst with molar ratio x=0.75 were excess from porous of ceria support. Obviously, the difference of

the mole ratio seems to be very significant. Ceria is very promising supporter, which allows the nickel oxides disperse on ceria surface.

The crystalline size of urea hydrolysis catalyst were distributed widely, i.e., 0.83 x 0.11 x 0.11 μm for molar ratio of x = 0.25 and 8.2 x 1.38 x 1.38 μm for molar ratio of x = 0.75. The fraction of microstructure with larger diameters increased as the loading amount of nickel in the catalyst became higher, will be because of the high loading amount of NiO, then NiO were react together then form NiO/NiO occur an amorphous structure and mix with crystalline structure phase .

Table 4.2 The range of crystalline size from SEM.

Samples		**Crystallite size width x length x high (μm)**
Co – precipitation method	$Ce_{0.75}Ni_{0.25}O_2$ (x = 0.25)	Amorphous
	$Ce_{0.25}Ni_{0.75}O_2$ (x = 0.75)	Amorphous
Urea hydrolysis method	$Ce_{0.75}Ni_{0.25}O_2$ (x = 0.25)	0.83 x 0.11 x 0.11
	$Ce_{0.25}Ni_{0.75}O_2$ (x = 0.75)	8.2 x 1.38 x 1.38

4.3 The characterization by the X-ray fluorescence (XRF)

Table 4.3 The elemental compositions of the catalysts.

Samples		**Elemental compositions (% wt.)***			**Theoretical molar ratio NiO : CeO_2**	**Actual molar ratio NiO : CeO_2**
		SiO_2	**NiO**	**CeO_2**		
Co – precipitation method	$Ce_{0.75}Ni_{0.25}O_2$	0.14	14.49	85.30	0.25 : 0.75	0.29 : 0.71
	$Ce_{0.25}Ni_{0.75}O_2$	0.28	56.70	43.01	0.75 : 0.25	0.76 : 0.24
Urea hydrolysis method	$Ce_{0.75}Ni_{0.25}O_2$	0.44	6.73	92.82	0.25 : 0.75	0.13 : 0.87
	$Ce_{0.25}Ni_{0.75}O_2$	1.47	54.16	44.37	0.75 : 0.25	0.70 : 0.30

* The elemental compositions were calculated by theoretical formulas, "fundamental parameter calculations".

From table 4.3, the X-ray fluorescence spectroscopy (XRF) showed the results of the elemental analysis of $Ce_{0.75}Ni_{0.25}O_2$ and $Ce_{0.25}Ni_{0.75}O_2$ mixed oxide catalysts prepared via co-precipitation and urea hydrolysis methods. The elemental compositions of the mixed oxide catalysts consisted of NiO and CeO_2. The actual molar ratio was quite close to the theoretical molar ratio of NiO : CeO_2. A few SiO_2 compositions were found due to the impurity from the preparation methods. The results were also supported by the X-ray diffraction (XRD) which showed both NiO and CeO_2 peaks.

4.4 The characterization by the X-ray diffractometer (XRD)

The $Ce_{1-x}Ni_xO_2$ mixed oxide catalysts which are calcined under the decided temperature and condition (calcination at the temperature of 550 °C) were characterized and identified the structure by the X-ray diffraction technique. Cu K_α radiation was used and the intensity data were collected at 25 °C over a 2θ range of 20 -80° with a scan speed of 5° (2θ)/ min and a scan step of 0.02° (2θ).

The diffraction patterns from the X-ray diffractometer were shown in the Fig. 4.5. The patterns were showed both NiO and CeO_2 peaks which related to the Table 4.3 from the X-ray fluorescence spectroscopy (XRF).

4.4.1 The comparison of the catalysts with the same preparation methods

Figure 4.5 (a-d) were shown the XRD patterns of the $Ce_{1-x}Ni_xO_2$ mixed oxide catalysts in the different molar ratio prepared via co – precipitation and urea hydrolysis methods, respectively. The peaks of ceria (CeO_2) at about 29, 33, and 48° represented the indices of (111), (200), and (220) planes, respectively [32]. This indicates a cubic fluorite structure and a single phase [27]. While the peaks at about 37, 43, and 62° are the peaks of NiO crystalline phase [32, 27].

At low Ni loading ($Ce_{1-x}Ni_xO_2$ when x = 0.25), no separate Ni and NiO phases were found for both catalysts prepared via co - precipitation and urea hydrolysis methods. This meant that NiO was already incorporated into CeO_2.

For higher Ni loading, the peak intensity was obviously stronger. It can be seen that CeO_2 improves the dispersion of NiO at lower loadings, while NiO existed in crystallized phase on the surface of $Ce_{1-x}Ni_xO_2$ when higher loading (x = 0.75). Noticed that when higher Ni loading both NiO and CeO_2 peaks were observed, this means that the catalysts became two-phases (NiO/ CeO_2) instead of the solid solution. This can also be seen from the SEM images (Fig.4.2 and 4.3).

4.4.2 The comparison of the catalysts with the different preparation methods

Fig. 4.5 (a-d) was shown the XRD patterns of the $Ce_{1-x}Ni_xO_2$ mixed oxide catalysts in the different preparation methods but with the same molar ratio which were x = 0.25 and 0.75, respectively. For urea hydrolysis method, the intensity of CeO_2 peaks was tended to be stronger than the peaks from co-precipitation method. So the catalysts prepared via urea hydrolysis method had more crystallinity which means that NiO had more probability to incorporate into CeO_2 than the catalysts prepared via co – precipitation method. This can be seen in the SEM images (Fig.4.2 and 4.3). In case of co – precipitation method, low intensity was shown; it meant that the catalysts were in amorphous phase which will be unstable at high temperature when testing the activity. And the broad peaks were shown which means that the particle sizes of the catalysts prepared via co – precipitation method were too small to be detected by the XRD technique.

Table 4.4 Lattice parameters and mean crystallite sizes of cubic phase (111) of $Ce_{1-x}Ni_xO_2$ (x = 0.25, 0.75) of both preparation methods.

Methods	Samples	Mean crystallite size (Å)	Lattice parameter (Å)
Co - precipitation	$Ce_{0.75}Ni_{0.25}O_2$ (x = 0.25)	85.8	2.805
	$Ce_{0.25}Ni_{0.75}O_2$ (x = 0.75)	99.5	2.752
Urea hydrolysis	$Ce_{0.75}Ni_{0.25}O_2$ (x = 0.25)	389.5	2.769
	$Ce_{0.25}Ni_{0.75}O_2$ (x = 0.75)	162.4	2.761

From Table 4.4, it can be seen that the lattice parameters of ceria decreased with the addition of Ni, suggesting that some Ni^{2+} ions were incorporated into the ceria lattice to form the solid solution of $Ce_{1-x}Ni_xO_2$, since the radius of Ni^{2+} ions (0.072 nm) is smaller than that of Ce^{4+} ions (0.101 nm) .The crystallite size of NiO in the $Ce_{1-x}Ni_xO_2$ mixed oxide catalysts can be calculated by using Scherer's equation (eq.2.8). The mean crystallite size of ceria decreased with increasing Ni content, indicating that Ni atoms incorporated into CeO_2 inhibit the crystal growth of ceria. XRD results showed that at least two types of Ni phase existed in the $Ce_{1-x}Ni_xO_2$ mixed oxide catalysts i.e. crystallized phase NiO on the surface of CeO_2, and Ni^{2+} ions incorporated into ceria lattice.

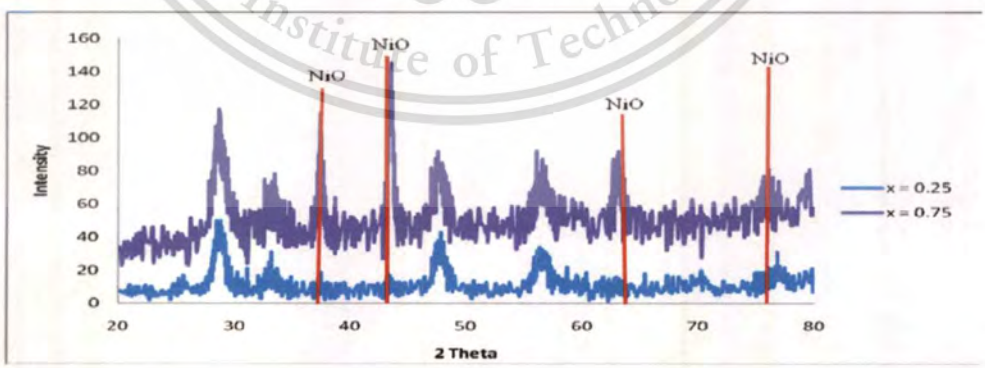

Figure 4.5 (a)

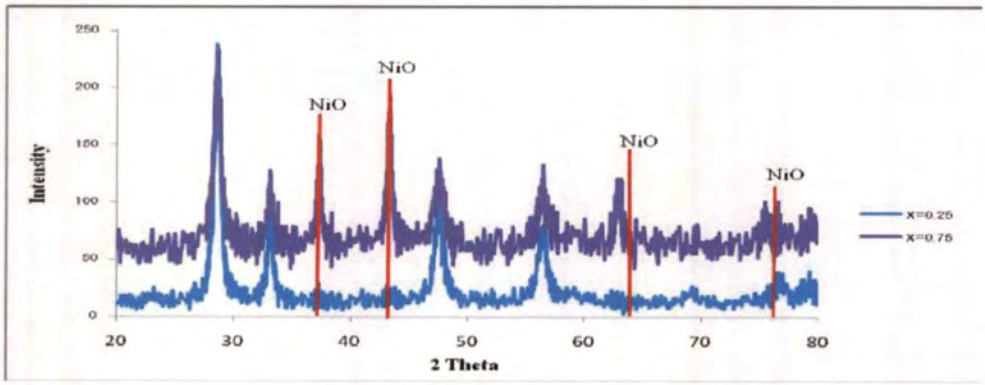

Figure 4.5 (b)

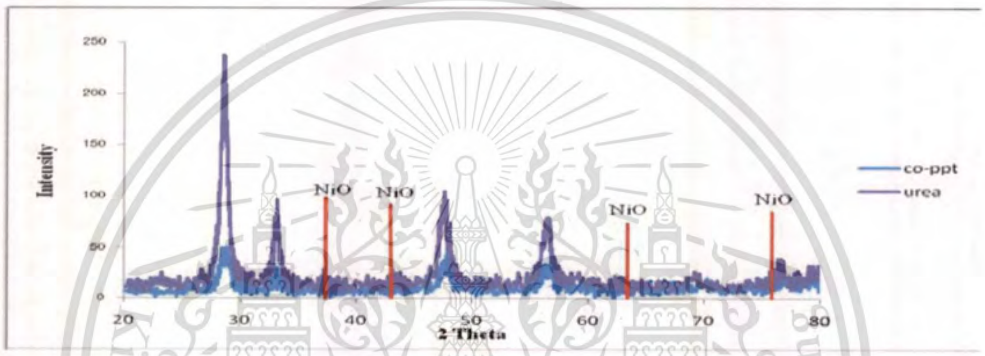

Figure 4.5 (c)

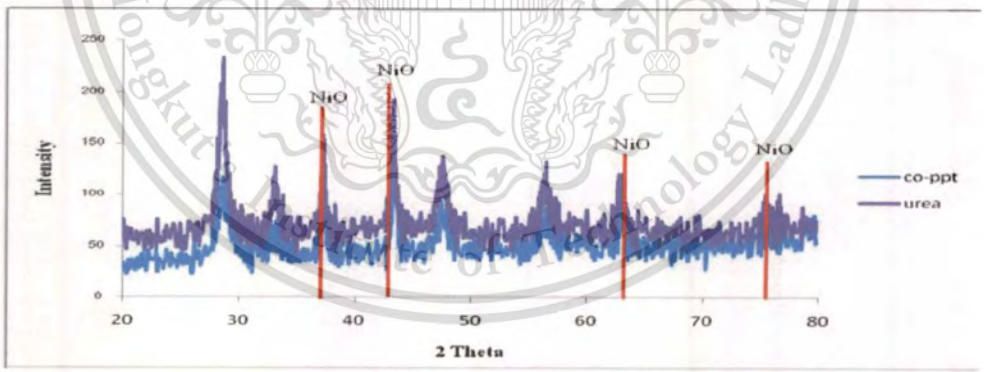

Figure 4.5 (d)

Figure 4.5 The XRD patterns of Ni over CeO_2 catalysts ($Ce_{1-x}Ni_xO_2$) after calcinations at 550 °C: (a) co – precipitation method with x = 0.25 and 0.75 (b) urea hydrolysis method with x = 0.25 and 0.75 (c) x = 0.25 with different preparation methods (d) x = 0.75 with different preparation methods.

4.5 The characterization by the H_2-Temperature programmed reduction (H_2-TPR)

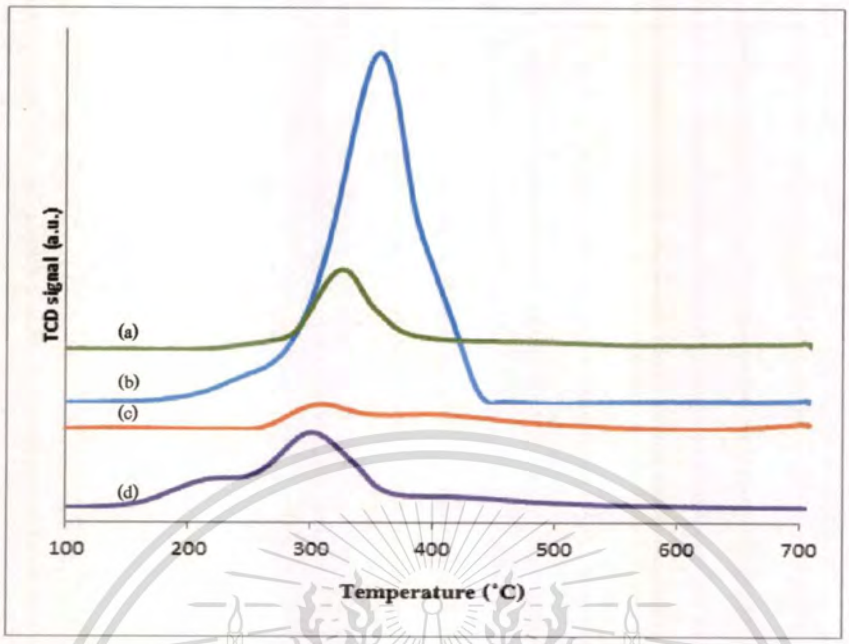

Figure 4.6 H_2-TPR profiles of catalysts calcined at 550 °C with a heating rate of 10 °C min^{-1}, a reducing gas containing 5% hydrogen in Argon with a flow rate of 50 ml min^{-1}: (a) $Ce_{0.75}Ni_{0.25}O_2$ via co-precipitation method, (b) $Ce_{0.25}Ni_{0.75}O_2$ via co-precipitation method, (c) $Ce_{0.75}Ni_{0.25}O_2$ via urea hydrolysis method and (d) $Ce_{0.25}Ni_{0.75}O_2$ via urea hydrolysis method.

The H_2-TPR profiles of the $Ce_{1-x}Ni_xO_2$ mixed oxide catalysts prepared via co-precipitation and urea hydrolysis methods are shown in Fig.4.6. The strong peak with maximum temperature at 360 °C was observed to be the reduction of NiO (indicated by XRD analysis) to Ni^0 [30]. It was indicated that the increasing in Ni loading did not have a significant effect on the reduction temperature of NiO over CeO_2. Small peaks with the maximum temperature at 250 °C were observed form the molar ratio x = 0.75 from both methods. They might be due to the reduction of free NiO particles from excess NiO or hydrogen spillover effect [30]. However, this small peak of co-precipitation method was smaller than the peak of urea hydrolysis method. It was suggested that NiO interactions in co-precipitation method were stronger than in urea hydrolysis method causing CeO_2 to be dominated in urea hydrolysis method. This was supported from the Table 4.3 which showed that the molar ratio of CeO_2 in the catalysts prepared via urea

hydrolysis method was higher than the catalysts prepared via co – precipitation method for x = 0.75.

The H_2-TPR profiles for the catalysts prepared via co-precipitation method were similar to those for the catalysts prepared via urea hydrolysis method as shown in Fig. 4.6. However, the reduction profile of the catalysts prepared via urea hydrolysis with molar ratio x=0.25 and x=0.75 was slightly different. The catalyst prepared via urea hydrolysis method with molar ratio x=0.75 showed a broader reduction peak than those prepared with molar ratio x=0.25. The wideness of the peak was due to a broad particle size distribution [30]. Hence, the crystalline size of the catalysts prepared via urea hydrolysis method was varied which related to the SEM technique. Likewise the reduction temperature of the catalysts prepared via co-precipitation was relatively higher than urea hydrolysis method. It was noticed that the reduction temperature of NiO from $Ce_{0.75}Ni_{0.25}O_2$ catalyst prepared via co-precipitation method was shifted from the maximum at 330 $^{\circ}$C to 310 $^{\circ}$ C when compared with NiO/CeO_2 catalyst with molar ratio x=0.25 prepared via urea hydrolysis method. This result indicated that the catalysts prepared via co-precipitation method had higher interaction between NiO and CeO_2 support [30].

Chapter 5

Conclusion and Recommendations

5.1 Conclusion

1. The thermogravimetric analysis data were used to determine changes in weight in relation to change in temperature. This can be designated the temperature range for the calcination of the $Ce_{1-x}Ni_xO_2$ mixed oxide catalysts. It showed that at the temperature over 550 °C, there was no weight loss shown in the diagram. It was postulated that at the temperature of 550 °C might be the lowest temperature for the calcination of $Ce_{1-x}Ni_xO_2$ mixed oxide catalysts.

2. From the X-ray fluorescence spectrometer (XRF), the result showed that the elemental compositions of the mixed oxide catalysts consisted of NiO and CeO_2. The actual molar ratio was quite close to the theoretical molar ratio of NiO : CeO_2.

3. The study of the factors that affected the catalysts after they were calcined was found from the X-ray diffraction technique (XRD):

- At low Ni loading ($Ce_{1-x}Ni_xO_2$ when x = 0.25), no separate Ni and NiO phases were found for both catalysts prepared via co - precipitation and urea hydrolysis methods. This meant that NiO was already incorporated into CeO_2.

- For higher Ni loading, the peak intensity was obviously stronger. It can be seen that CeO_2 improves the dispersion of NiO at lower loadings, while NiO existed in crystallized phase on the surface of $Ce_{1-x}Ni_xO_2$ when higher loading (x = 0.75).

- For urea hydrolysis method, the intensity of CeO_2 peaks was tended to be stronger than the peaks from co-precipitation method. So the catalysts prepared via urea hydrolysis method had more crystallinity which means that NiO had more probability to incorporate into CeO_2 than the

catalysts prepared via co – precipitation method. This can be seen in the SEM images (Fig.4.2 and 4.3).

- The lattice parameters of ceria decreased with the addition of Ni, suggesting that some Ni^{2+} ions were incorporated into the ceria lattice to form the solid solution of $Ce_{1-x}Ni_xO_2$, since the radius of Ni^{2+} ions (0.072 nm) is smaller than that of Ce^{4+} ions (0.101 nm).

- The mean crystallite size of ceria decreased with increasing Ni content, indicating that Ni atoms incorporated into CeO_2 inhibit the crystal growth of ceria.

4. The SEM images showed that the catalysts prepared via co-precipitate method were observed amorphous structure, and for catalysts prepared via urea hydrolysis method were observed crystalline structure. The catalysts which have higher molar ratio tended to be an amorphous phase by excess NiO. Hence, to prepare a good catalyst, urea hydrolysis is better method; the mole ratio should not be too high.

5. The temperature programmed reduction (TPR) technique identifies the most efficient reduction conditions, the supported precursor phases and their interactions with the support. It was indicated that the increasing in Ni loading did not have a significant effect on the reduction temperature of NiO over CeO_2. The catalyst prepared via urea hydrolysis method showed a broader reduction peak than those prepared via co-precipitation method. Hence, the crystalline size of the catalysts prepared via urea hydrolysis method was varied which related to the SEM technique. It was noticed that the reduction temperature of NiO from $Ce_{0.75}Ni_{0.25}O_2$ mixed oxide catalyst prepared via co-precipitation method was shifted from the maximum at 330 °C to 310 °C when compared with the catalyst prepared via urea hydrolysis method. This result indicated that the catalysts prepared via co-precipitation method had higher interaction between NiO and CeO_2 support.

6. The $Ce_{1-x}Ni_xO_2$ mixed oxide catalysts when x=0.75 had the Ni excess which shown into two phases in the XRD result. And from SEM result, their structure was the amorphous. Hence, these catalysts cannot be the $Ce_{0.25}Ni_{0.75}O_2$ mixed oxide solid solution but instant it became NiO/CeO_2.

5.2 Recommendations

1. This experiments should be done in the closed system to prevent the other impurities.

2. The calcinations temperature and the mole ratio of the catalysts should be varied to further study the structure and the factors which affect the catalysts' properties.

3. The characterization technique should be included the BET method to study the surface area of the catalysts.

4. The catalysts should be tested on the activity to study their efficiency.

5. The catalysts should be characterized with the FTIR technique to find the elements which were decomposed for support the TGA results.

References

[1] http://www.enviroliteracy.org/subcategory.php/21.html

[2] A.M. Silva, L.O.O. Costa, A.P.M.G. Barandas, L.E.P. Borges, L.V. Mattos, F.B. Noronha. **Effect of the metal nature on the reaction mechanism of the partial oxidation of ethanol over CeO_2-supported Pt and Rh catalysts.** Catalysis Today 133–135 (2008) 755–761.

[3] Xu S., Wang X. **Highly active and coking resistant Ni/CeO_2–ZrO_2 catalyst for partial oxidation of methane.** Fuel 84 (2005) 563 – 567.

[4] B. Koubaissy,A. Pietraszek, A.C. Roger, A. Kiennemann. **CO_2 reforming of methane over Ce – Zr – Ni – Me mixed catalysts.**Catalysis today (2010).

[5] Pengpanich S., Vissanu M., Rirksomboon T. **Catalytic oxidation of methane over CeO_2 – ZrO_2 mixed oxide solid solution catalysts prepared via urea hydrolysis.** Applied catalysis A: General 234 (2002) 221 – 233.

[6] K. Otsuka, W. Ye, M. Nakamura, Appl. Catal. A 183 (1999) 317.

[7] A. Trovarelli, C. de Leitenburg, M. Boaro, G. Dolcetti, Catal.Today 50 (1999) 353.

[8] http://en.wikipedia.org/wiki/Cerium(IV)_oxide

[9] http://www.thegeminigeek.com/what-is-catalyst/

[10] http://en.wikipedia.org/wiki/Catalysis

[11] James J. Spivey. **Catalysis number10 ofSpecialist Periodical Reports**. James J. Spivey, S. K. Agarwal : Royal Society of Chemistry, 1993.

[12] http://en.wikipedia.org/wiki/Cerium%28IV%29_oxide

[13] http://www.lenntech.com/periodic/elements/ni.htm#ixzz0xcqDNPgp

[14] http://www.freepatentsonline.com/4005031.html

[15] http://www.cee.vt.edu/ewr/environmental/teach/gwprimer/group01/ Precip. Html

[16] JingHe, MinWei, BoLi, YuKang, DavidGEvans, XueDuan. "Preparation of Layered Double Hydroxides".Struct Bond (2006) 119: 89–119.

[17] http://physicalchemistryresources.com/Book5_sectionsBook5_sections/TA_Thermogravimetric %20AnalysisHTML_1.ht

[18] areeweb.polito.it/ricerca/carbongroup/fac_tga.html

[19] http://mee-inc.com/sem.html

[20] http://materialscience.uoregon.edu/ttsem/SEMbasics.html

[21] http://www.itnes.com/x.php?page=13

[22] http://www.rigakuedxrf.com

[23] webmineral.com/help/**XRay**Diffraction.shtml

[24] http://www.tulane.edu/~sanelson/eens211/x-ray.htm

[25] http://www.ceinstruments.co.uk/tprtpo.html

[26] www.vscht.cz/kat/download/lab_**tpr**_eng.doc

[27] Yong Li, Baocai Zhang, Xiaolan Tang, YideXu, WenjieShen. **"Hydrogen production from methane decomposition over Ni/CeO_2 catalysts".** Catalysis Communications 7 (2006) 380–386.

[28] J.A. Montoya, E. Romero-Pascual, C. Gimonc, P. Del Angel a, A. Monzónb.**"Methane reforming with CO_2 over Ni/ZrO_2–CeO_2 catalysts prepared by sol–gel".** Catalysis Today 63 (2000) 71–85.

[29] Leung P. Tanga, Louise Diamonda, Marion MacDonalda, Brian G. McMillana, James Morrowa, Mark D. Spicera, Le´onard E.A. Berlouisa,*, Michael Westonb. **"Impact of synthesis temperature on hydrogen storage and emission from Ni/Ce composite oxides".**International journal of hydrogen energy 34 (2009) 7296-7305.

[30] SitthiphongPengpanich a, VissanuMeeyoo b,*, ThirasakRirksomboon a. **"Methane partial oxidation over Ni/CeO_2–ZrO_2 mixed oxide solid solution catalysts".**Catalysis Today 93–95 (2004) 95–105.

[31] Tianli Zhu, Maria Flytzani – Stephanopoulos. **"Catalytic partial oxidation of methane to synthesis gas over Ni-CeO_2".** Applied catalysis A: General 208 (2001) 403 – 417.

[32] Maria D. Salazar – Villalpando and Bryan Reyes. **"Hydrogen production over Ni/ceria-supported catalysts by partial oxidation of methane".**International journal of hydrogen energy 34 (2009) 9723 – 9729.

[33] MeilingTeng, LaitaoLuo, Xiaomao Yang. **"Synthesis of mesoporous $Ce_{1-x}Zr_xO_2$ (x = 0.2 – 0.5) and catalytic properties of CuO based catalysts".**Microporous and mesoporous materials 119 (2009) 158 – 164.

[34] NavadolLaosiripojana, SuttichaiAssabumrungrat, SumittraCharojrochkul. **"Catalytic cracking of methane, methanol, and ethanol by ceria".**The joint international conference on Sustainable energy and Environment (SEE) 1-3 December 2004, HuaHin, Thailand.

[35] D. Srinivas, C.V.V. Satyanarayana, H.S. Potdar, P.Ratnasamy. **"Structural studies on NiO-CeO_2-ZrO_2 catalysts for steam reforming of ethanol".** Applied catalysis A: General 246 (2003) 323-334.

[36] SitthiphongPengpanich, VissanuMeeyoo, ThirasakRirksomboon, KunchanaBunyakiat. **"Catalytic oxidation of methane over CeO_2 – ZrO_2 mixed oxide solid solution catalysts prepared via urea hydrolysis".** Applied catalysis A: General 234 (2002) 221 – 233.

Appendix A

Table from the calculations

1. The preparation by the co – precipitation method

x	0.1M $Ce(NO_3)_3 \cdot 6H_2O$ solution		0.1M $Ni(NO_3)_2 \cdot 6H_2O$ solution		0.1M NaOH solution		Weight of $Ce_{1-x}Ni_xO_2$ (g)
	Weight of $Ce(NO_3)_3 \cdot 6H_2O$ (g)	Volume of distilled water (ml)	Weight of $Ni(NO_3)_2 \cdot 6H_2O$ (g)	Volume of distilled water (ml)	Weight of NaOH (g)	Volume of distilled water (ml)	
0.25	6.5132	150	1.4539	50	3.9997	1000	2.9552
0.75	2.8947	67	5.8157	200			2.6412

2. The preparation by the urea hydrolysis method

x	0.1M $Ce(NO_3)_3 \cdot 6H_2O$ solution		0.1M $Ni(NO_3)_2 \cdot 6H_2O$ solution		0.4M urea solution $(NH_2)_2CO$		Weight of $Ce_{1-x}Ni_xO_2$ (g)
	Weight of $Ce(NO_3)_3 \cdot 6H_2O$ (g)	Volume of distilled water (ml)	Weight of $Ni(NO_3)_2 \cdot 6H_2O$ (g)	Volume of distilled water (ml)	Weight of $(NH_2)_2CO$ (g)	Volume of distilled water (ml)	
0.25	5.2106	120	1.1632	40	1.9218	80	2.3641
0.75	1.7369	40	3.4895	120			1.5848

Appendix B

1. Preparation by the co - precipitation method

1.1 Preparation of $Ce_{1-x}Ni_xO_2$ when x = 0.25

Basis: Distilled water needed for dilution of Ce $(NO_3)_3 \cdot 6\ H_2O$ is 150 ml

1.1.1 The calculation formula for the weight of 0.1M Ce $(NO_3)_3 \cdot 6\ H_2O$

$$wt\ of\ Ce(NO_3)_3 \cdot 6H_2O = \frac{distilled\ water\ used \times molar\ ratio \times Mw\ of\ Ce(NO_3)_3 \cdot 6H_2O}{vol.of\ distilled\ water}$$

1.1.2 The calculation formula for the weight of CeO_2

$$wt.of\ CeO_2 = \frac{wt.of\ Ce(NO_3)_2 \cdot 6H_2O \times Mw\ of\ CeO_2}{Mw\ of\ Ce(NO_3)_2 \cdot 6H_2O}$$

1.1.3 The calculation formula for the weight of NiO

$$wt.of\ NiO = \frac{mol\ of\ CeO_2 \times molar\ ratio(x=0.25)}{1-x} \times Mw\ of\ NiO$$

1.1.4 The calculation formula for the weight of 0.1M Ni $(NO_3)_2 \cdot 6\ H_2O$

$$wt\ of\ Ni(NO_3)_2 \cdot 6H_2O = \frac{wt\ of\ NiO}{mw\ of\ NiO} \times Mw\ of\ Ni(NO_3)_2 \cdot 6H_2O$$

1.1.5 The calculation formula for the volume of distilled water used for dilution

0.1M Ni $(NO_3)_2 \cdot 6\ H_2O$

$$distilled\ water\ used = \frac{wt.of\ Ni(NO_3)_2 \times vol.of\ distilled\ water}{molarity \times Mw\ of\ Ni(NO_3)_2}$$

\

1.2 Preparation of $Ce_{1-x}Ni_xO_2$ when x = 0.75

Basis: Distilled water needed for dilution of Ni $(NO_3)_2 \cdot 6\,H_2O$ is 200 ml

1.2.1 The calculation formula for the weight of 0.1M Ni $(NO_3)_2 \cdot 6\,H_2O$

$$wt\ of\ Ni(NO_3)_2 \cdot 6H_2O = \frac{distilled\ water\ used \times molar\ ratio \times Mw\ of\ Ni(NO_3)_2 \cdot 6H_2O}{vol.of\ distilled\ water}$$

1.2.2 The calculation formula for the weight of NiO

$$wt.of\ NiO = \frac{wt.of\ Ni(NO_3)_2 \cdot 6H_2O \times Mw\ of\ NiO}{Mw\ of\ Ni(NO_3)_2 \cdot 6H_2O}$$

1.2.3 The calculation formula for the weight of CeO_2

$$wt.of\ CeO_2 = \frac{mol\ of\ NiO \times (1-x)}{molar\ ratio(x=0.75)} \times Mw\ of\ CeO_2$$

1.2.4 The calculation formula for the weight of 0.1M Ce $(NO_3)_3 \cdot 6\,H_2O$

$$wt\ of\ Ce(NO_3)_3 \cdot 6H_2O = \frac{wt\ of\ CeO_2}{mw\ of\ CeO_2} \times Mw\ of\ Ce(NO_3)_3 \cdot 6H_2O$$

1.2.5 The calculation formula for the volume of distilled water used for dilution 0.1M Ce $(NO_3)_3 \cdot 6\,H_2O$

$$distilled\ water\ used = \frac{wt.of\ Ce(NO_3)_3 \times vol.of\ distilled\ water}{molarity \times Mw\ of\ Ce(NO_3)_3}$$

1.3 The calculation formula of the weight of $Ce_{1-x}Ni_xO_2$

$$wt\ of\ Ce_{1-x}Ni_xO_2 = \text{wt of } CeO_2 + \text{wt of NiO}$$

1.4 The calculation formula for the preparation of 0.1M NaOH solution

$$wt.of\ NaOH = \frac{disired\ distilled\ water \times molarity \times Mw\ of\ NaOH}{distilled\ water\ used}$$

2. Preparation by the urea hydrolysis method

2.1 The calculation formula for the weight of 0.1M Ce $(NO_3)_3 \cdot 6\ H_2O$

$$wt.of\ Ce(NO_3)_3 \cdot 6H_2O = \frac{[Mw\ of\ Ce(NO_3)_3 \cdot 6H_2O] \cdot (Molarity) \cdot (1-x)(Volume\ of\ Ce(NO_3)_3 \cdot 6H_2O)}{1000}$$

2.2 The calculation formula for the weight of 0.1M Ni $(NO_3)_2 \cdot 6\ H_2O$

$$wt.of\ Ni(NO_3)_2 \cdot 6H_2O = \frac{[Mw\ of\ Ni(No_3)_2 \cdot 6H_2O] \cdot (Molarity) \cdot (x)(Volume\ of\ Ni(No_3)_2 \cdot 6H_2O)}{1000}$$

2.3 The calculation formula for the weight of CeO_2

$$wt.of\ CeO_2 = \frac{wt.of\ Ce(No_3)_3 \cdot 6H_2O}{Mw\ of\ Ce(No_3)_3 \cdot 6H_2O} \times Mw\ of\ CeO_2$$

2.4 The calculation formula for the weight of NiO

$$wt.of\ NiO = \frac{wt.of\ Ni(No_3)_2 \cdot 6H_2O}{Mw\ of\ Ni(No_3)_2 \cdot 6H_2O} \times Mw\ of\ NiO$$

2.5 The calculation formula of the weight of $Ce_{1-x}Ni_xO_2$

$$wt\ of\ Ce_{1-x}Ni_xO_2 = \text{wt of } CeO_2 + \text{wt of NiO}$$

2.6 The calculation formula for the preparation of 0.4M urea solution with 2:1 v/v

$$weight\ of\ urea\ ((NH_2)_2CO) = \frac{mw\ of\ urea \times molarity \times vol.of\ distilled\ water}{1000}$$

Appendix C

Physical characteristics of catalyst before calcine and after calcine

Table A.1 Catalyst prepared by co-precipitate method.

Molar ratio	Before calcine	After calcine
$Ce_{0.75}Ni_{0.25}O_2$		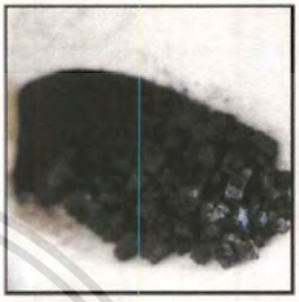
$Ce_{0.25}Ni_{0.75}O_2$		

Table A.2 Catalyst prepared by urea hydrolysis method.

Molar ratio	Before calcine	After calcine
$Ce_{0.75}Ni_{0.25}O_2$		
$Ce_{0.25}Ni_{0.75}O_2$